

Molecular Docking Screens Using Comparative Models of Proteins

Hao Fan,^{†,‡} John J. Irwin,[‡] Benjamin M. Webb,[†] Gerhard Klebe,[§] Brian K. Shoichet,^{*,‡} and Andrej Sali^{*,†}

Department of Bioengineering and Therapeutic Sciences, Department of Pharmaceutical Chemistry, and California Institute for Quantitative Biosciences, University of California at San Francisco, San Francisco, California 94158, Department of Pharmaceutical Chemistry and California Institute for Quantitative Biosciences, University of California at San Francisco, San Francisco, California 94158, and Institute of Pharmaceutical Chemistry, University of Marburg, Marburg, Germany

Received September 25, 2009

Two orders of magnitude more protein sequences can be modeled by comparative modeling than have been determined by X-ray crystallography and NMR spectroscopy. Investigators have nevertheless been cautious about using comparative models for ligand discovery because of concerns about model errors. We suggest how to exploit comparative models for molecular screens, based on docking against a wide range of crystallographic structures and comparative models with known ligands. To account for the variation in the ligand-binding pocket as it binds different ligands, we calculate “consensus” enrichment by ranking each library compound by its best docking score against all available comparative models and/or modeling templates. For the majority of the targets, the consensus enrichment for multiple models was better than or comparable to that of the holo and apo X-ray structures. Even for single models, the models are significantly more enriching than the template structure if the template is paralogous and shares more than 25% sequence identity with the target.

INTRODUCTION

Structure-based methods have been widely used in ligand design and discovery.^{1–4} In particular, ligands can be identified among a large library of small molecules by virtual screening.^{1,5–11} Each library molecule is docked into a binding site, then scored and ranked by its complementarity to the protein. High-ranking docked molecules are subsequently tested experimentally. The two critical parts of this process are the docking to search through plausible binding modes for candidate compounds and the scoring to distinguish ligands from nonbinding “decoys”.

Docking a ligand to a protein structure is most successful when the shape of the binding site is similar to that found in the protein–ligand complex. Therefore, the protein structure for docking is best determined in complex with a ligand that is similar to the ligand being docked, by X-ray crystallography or NMR spectroscopy. Induced fit and differences between conformations of the protein bound to different ligands limit the utility of the unbound structure (apo structure) and even complex structures (holo structures) obtained for dissimilar ligands. The problem of the protein conformational heterogeneity is especially difficult to surmount in virtual screening, which involves docking of many different ligands, each one of which may in principle bind to a different protein conformation.

An even greater challenge is that many interesting targets have no experimentally determined structures at all, especially in the early phases of ligand discovery. During the last five years, the number of experimentally determined structures deposited in the Protein Data Bank (PDB) increased from 23 096 to 52 821 (September 2008).¹² However, over the same period, the number of sequences in the Universal Protein Resource (UniProt) increased from 1.2 million to 6.4 million.^{13,14} This rapidly growing gap between the sequence and structure databases can be bridged by protein structure prediction,¹⁵ including comparative modeling, threading, and de novo methods. Despite progress in de novo prediction,^{16,17} comparative modeling remains the most reliable method that can sometimes predict the structure of a protein with an accuracy comparable to a low-resolution, experimentally determined structure.¹⁸ Comparative modeling benefits from structural genomics.¹⁹ In particular, the Protein Structure Initiative (PSI) aims to determine representative atomic structures of most major protein families by X-ray crystallography or NMR spectroscopy, so that most of the remaining protein sequences can be characterized by comparative modeling (<http://www.nigms.nih.gov/Initiatives/PSI/>).^{20,21} Currently, the fraction of sequences in a genome for whose domains comparative models can be obtained varies from approximately 20% to 75%, increasing the number of structurally characterized protein sequences by 2 orders of magnitude relative to the entries in the PDB.¹⁴ Therefore, comparative models in principle greatly extend the applicability of virtual screening, as compared to using only the experimentally determined structures.²²

Comparative models have in fact been used in virtual screening to detect novel ligands for many protein targets,²²

* Corresponding author phone: (415) 514-4227 (A.S.), (415) 514-4126 (B.K.S.); fax: (415) 514-4231 (A.S.), (415) 514-4260 (B.K.S.); e-mail: sali@salilab.org (A.S.); shoichet@cgl.ucsf.edu (B.K.S.).

[†] Department of Bioengineering and Therapeutic Sciences, Department of Pharmaceutical Chemistry, and California Institute for Quantitative Biosciences, University of California at San Francisco.

[‡] Department of Pharmaceutical Chemistry and California Institute for Quantitative Biosciences, University of California at San Francisco.

[§] Institute of Pharmaceutical Chemistry, University of Marburg.

including the G-protein coupled receptors (GPCR),^{23–35} protein kinases,^{36–39} nuclear hormone receptors, and several different enzymes.^{40–53} Nevertheless, the relative utility of comparative models versus experimentally determined structures has only been sparsely assessed.^{23,36,37,54–56} In a study of 10 enzyme targets, the X-ray structure of a ligand-bound target often provided the best enrichment for known binders.⁵⁶ The comparative models yielded better enrichment than random selection and performed comparably to the holo X-ray structure in two cases. The relationship between the sequence identity on which a model is based and the screening accuracy was addressed by virtual screening against eight and four comparative models for factor VIIa and cyclin-dependent kinase 2 (CDK2), respectively.³⁷ It was shown that a 5-fold enrichment over random selection was obtained using comparative models based on templates with sequence identities greater than 50%. In an intriguing study, Gilson and co-workers observed that, whereas docking against comparative models could lead to substantial enrichment,⁵⁵ there was little correlation between target–template sequence identity and the success of the docking screen. Furthermore, the templates on which the modeled structures were based (i.e., proteins with putatively incorrect sequences) could perform just as well in the docking screens, as the comparative models built from them with the correct sequence.

The lack of consensus in these observations, and arguably the absence of a large-scale benchmarking study, inspired us to investigate the following questions. How does docking against comparative models compare to random selection and to docking against the template structures, over a large number of proteins? If multiple models are calculated on the basis of different templates, can any of them outperform apo and even holo X-ray structures of the target? If so, can one reliably identify which model will do so, or even perform optimally among a set of modeled structures; are there sequence and/or structural attributes (i.e., the overall target–template sequence identity, the binding site target–template sequence identity, and the predicted accuracy of a model) that reliably predict the accuracy of ligand docking? Can the docking screens be improved by employing multiple models, or will using multiple models merely increase the noise from decoys?

Here, we answered these questions with the aid of 38 protein targets selected from the “directory of useful decoys” (DUD).⁵⁷ For each target, DUD contains known ligands as well as decoys with similar physical properties but dissimilar chemical structures. Our analysis proceeded in three steps, performed independently for each of the 38 targets. First, comparative models were calculated on the basis of different template structures. Second, all compounds in DUD were docked against the holo and apo (if available) X-ray structure of the target, the comparative models, and the template X-ray structures. Third, the docking was evaluated on the basis of the enrichment for known ligands with respect to the whole DUD. The enrichments achieved with modeled structures were compared to those achieved with X-ray structures of the corresponding target and templates. We correlate the success of docking with a variety of target/template attributes. In addition, we evaluated a consensus enrichment that combines docking scores from independent virtual screens against different comparative models of the same target.

We begin by describing the target set, the automated modeling and docking pipeline, and methods to evaluate the model accuracy, to evaluate the accuracy of virtual ligand screening, and to compare ligand enrichments yielded by different structures (Methods). We then describe the relative utilities of comparative models and X-ray structures for virtual screening, as well as the correlation between the screening performance and various template/model/target similarity measures (Results). Finally, we discuss the implications of the current approach and answer the questions we asked above, given our modeling, docking, and benchmark (Discussion and Conclusions).

METHODS

Target Set. DUD contains 2950 annotated ligands and 95 316 corresponding decoys for 40 protein targets.⁵⁷ Here, we used the 38 targets of DUD for which holo X-ray structures are available in the PDB (Table 1). These targets are organized into two classes: enzymes (six of which are kinases) and nuclear hormone receptors. For each target, the holo X-ray structure in the original study of DUD was used, except for androgen receptor for which a more recently deposited structure was selected (PDB ID 2ao6). An apo structure with the highest sequence identity to the holo structure was also used; no apo structure was found for four hormone receptors. For each target sequence, templates for comparative modeling were obtained from the PDB. We aimed to include one holo and one apo template structure for each of the eight 10% sequence identity ranges from 20% to 100%. Structural alignments were performed with the MAMMOTH program⁵⁸ via the DBALI server.⁵⁹

Comparative Modeling. For each target–template pair, a comparative model was generated using MODELLER-9v2.⁶⁰ The target–template alignment was calculated by profile–profile alignment as implemented in the “profile.scan” routine of MODELLER.⁶¹ For each alignment, 50 models were calculated with the standard “automodel” class. Next, the binding site loops were defined as those binding site residues that were not aligned to the template structure; the binding site residues, in turn, were defined as the residues with more than one non-hydrogen atom within 10 Å of any ligand atom in the target structure. The model with the best MODELLER objective function value was then subjected to a refinement of binding site loops with the standard “loopmodel” class; all of the binding site loops were optimized simultaneously. 2500 target conformations were generated, and the single refined model with the best objective function value was selected for virtual screening. Ligands, ions, and cofactors in the templates were copied to the target models and treated as rigid during both initial model building and binding site refinement, using the “BLK” functionality of MODELLER. In total, 222 models were generated on the basis of 222 templates for the 38 test proteins (Table S3). 172 of the 222 templates are determined by X-ray crystallography at resolution better than 2.5 Å.

Evaluation of Comparative Models. The comparative models were assessed by the root-mean-square deviation of the non-hydrogen atoms in binding site residues between a model and the holo X-ray structure (RMSD_{bs}), after superposition of the binding site atoms by MODELLER’s “superpose” routine. The holo X-ray structures and comparative models were also assessed by an atomic distance-

Table 1. Protein Targets for Virtual Ligand Screening^a

protein target	PDB code (holo)	PDB code (apo)	number of ligands	sequence identity of templates [%]	number of templates (holo)	number of templates (apo)
ACE	1o86	2iul	49	42–55	3	1
ADA	1ndw	1vfl	23	26–85	1	1
COMT	1h1d	2avd	12	20	1	0
PDE5	1xp0	2h40	51	24–96	2	2
DHFR	3dfr	1zdr	201	20–37	5	3
GART	1c2t	3gar	21	40–42	1	1
FXa	1f0r	1c5m	142	24–64	3	4
thrombin	1ba8	2afq	65	23–40	3	3
trypsin	1bjv	2tga	44	21–79	5	5
AChE	1eve	1qih	105	28–93	4	4
ALR2	1ah3	1xgd	26	20–87	5	6
AmpC	1xgj	1l0d	21	20–77	3	4
COX-1	1q4g	1prh	25	62–63	1	1
COX-2	1cx2	5cox	349	64–65	1	1
GPB	1a8i	1gpb	52	42–81	2	0
HIVPR	1hpx	3phv	53	23–97	7	5
HIVRT	1rt1	1rtj	40	98–99	1	1
HMGR	1hw8	1r7i	35	100	2	0
InhA	1p44	2ied	85	20–29	2	2
NA	1a4g	1nsb	49	29–34	2	1
PARP	1efy	2paw	33	46–87	1	1
PNP	1b8o	1pbn	25	20–93	5	3
SAHH	1a7a	1ky4	33	49–85	2	0
CDK2	1ckp	1hcl	50	21–95	6	6
EGFr	1m17	1m14	444	20–38	3	3
FGFr1	1agw	1fgk	118	20–51	4	4
HSP90	1uy6	1uyl	24	20–70	5	3
P38 MAP	1kv2	1p38	256	20–62	5	4
SRC	2src	1fmk	162	20–82	7	4
TK	1kim	1e2h	22	21–40	3	0
AR	2ao6		74	20–84	5	1
ER _{agonist}	1l2i	2b23	67	20–93	7	2
ER _{antagonist}	3ert	2b23	39	21–93	6	3
GR	1m2z		78	22–56	6	1
MR	2aa2		15	20–57	3	1
PPAR _g	1fm9	1prg	81	20–65	3	2
PR	1sr7		27	20–54	4	1
RXR _α	1mvc	1glu	20	20–89	5	4

^a Protein target: ACE, angiotensin-converting enzyme; ADA, adenosine deaminase; COMT, catechol *O*-methyltransferase; PDE5, phosphodiesterase 5; DHFR, dihydrofolate reductase; GART, glycinamide ribonucleotide transformylase; FXa, factor Xa; AChE, acetylcholinesterase; ALR2, aldose reductase; AmpC, AmpC β -lactamase; COX-1, cyclooxygenase-1; COX-2, cyclooxygenase-2; GPB, glycogen phosphorylase beta; HIVPR, HIV protease; HIVRT, HIV reverse transcriptase; HMGR, hydroxymethylglutaryl-CoA reductase; InhA, enoyl ACP reductase; NA, neuraminidase; PARP, poly(ADP-ribose) polymerase; PNP, purine nucleoside phosphorylase; SAHH, S-adenosyl-homocysteine hydrolase; CDK2, cyclin-dependent kinase 2; EGFr, epidermal growth factor receptor kinase domain; FGFr1, fibroblast growth factor receptor kinase; HSP90, human heat shock protein 90; P38 MAP, P38 mitogen activated protein; SRC, tyrosine kinase SRC; TK, thymidine kinase; AR, androgen receptor; ER, estrogen receptor; GR, glucocorticoid receptor; MR, mineralocorticoid receptor; PPAR_g, peroxisome proliferator activated receptor gamma; PR, progesterone receptor; RXR_α, retinoic X receptor alpha. PDB code (holo), the X-ray structure of the protein target with a bound ligand. Number of ligands, the number of annotated binders of the protein target in the database. Sequence identity of templates, the range of sequence identity from all templates with respect to the holo X-ray structure of the protein target. Number of templates (holo), the number of template structures cocrystallized with a ligand.

dependent statistical potential called discrete optimized protein energy (DOPE).⁶² The normalized score (N-DOPE) derived from the raw DOPE score was used.⁶³ The N-DOPE score can often discriminate between near-native (native overlap “NO3.5 Å” > 0.8; N-DOPE < −1.0) and inaccurate models (NO3.5 Å < 0.3; N-DOPE > 1.0).

Molecular Docking. DUD ligands and decoys (98 266 molecules) were screened against the holo X-ray structure, the apo X-ray structure, the comparative models, and the template X-ray structures of each target. The apo X-ray structure, the comparative models, and the template structures were superposed on the corresponding holo X-ray structure using the binding site residues only (for template structures, the residues aligned to the binding site residues were used). Virtual screening against the 38 holo X-ray structures, 34

apo X-ray structures, 222 comparative models, and 222 template structures was performed using a semiautomated docking pipeline.⁵⁷ Briefly, the protocol includes binding site preparation, sphere (hot spot) generation, scoring grids construction, and docking of DUD. The solvent-accessible molecular surface was calculated for the binding site residues using the program DMS.⁶⁴ For the holo X-ray structure, 35 matching spheres serving to orient DUD compounds in the site were generated by augmenting the ligand-derived spheres with the receptor-derived spheres. The ligand-derived spheres were represented by the positions of non-hydrogen atoms of the ligand in the holo X-ray structure. The receptor-derived spheres were calculated using the program SPHGEN⁶⁵ from the molecular surface of the binding site. The matching spheres generated in the holo X-ray structures were employed

for the corresponding apo X-ray structures, the comparative models, and the template structures. The program DOCK 3.5.54 was used for docking.^{66–68} Presampled conformations of each compound were docked to the binding site and ranked by an energy function consisting of protein–ligand van der Waals interactions, protein–ligand electrostatic interactions, and a correction for ligand desolvation.

Evaluation of Virtual Screening Results. The accuracy of virtual screening was evaluated by the enrichment for the known ligands among the top scoring DUD compounds. The conformation with the best docking energy of each compound was ranked, and the enrichment factor was defined as

$$EF_{\text{subset}} = \frac{(\text{ligand}_{\text{selected}}/N_{\text{subset}})}{(\text{ligand}_{\text{total}}/N_{\text{total}})} \quad (1)$$

where $\text{ligand}_{\text{total}}$ is the number of known ligands in a database containing N_{total} compounds, and $\text{ligand}_{\text{selected}}$ is the number of ligands found in a given subset of N_{subset} compounds. EF_{subset} reflects the ability of virtual screening to find true positives among the decoys in the database as compared to a random selection. An enrichment curve is obtained by plotting the percentage of actual ligands found (y-axis) within the top ranked subset of all database compounds (x-axis on logarithmic scale). To measure the enrichment independently of the arbitrary value of N_{subset} , we also calculated the area under the curve (logAUC) of the enrichment plot:

$$\log\text{AUC} = \frac{1}{\log_{10} 100/0.1} \sum_{0.1}^{100} \frac{\text{ligand}_{\text{selected}}(x)}{\text{ligand}_{\text{total}}} \Delta x \text{ and } x = \log_{10} \frac{N_{\text{subset}}}{N_{\text{total}}} \quad (2)$$

where Δx is 0.1 in this study. A random selection ($\text{ligand}_{\text{selected}}/\text{ligand}_{\text{total}} = N_{\text{subset}}/N_{\text{total}}$) of compounds from the mixture of actual ligands and decoys yields a logAUC of 14.5. A mediocre selection that picks twice as many ligands at any N_{subset} as a random selection has logAUC of 24.5 ($\text{ligand}_{\text{selected}}/\text{ligand}_{\text{total}} = 2 * N_{\text{subset}}/N_{\text{total}}$; $N_{\text{subset}}/N_{\text{total}} \leq 0.5$). A highly accurate enrichment that produces 10 times as many ligands as the random selection has logAUC of 47.7 ($\text{ligand}_{\text{selected}}/\text{ligand}_{\text{total}} = 10 * N_{\text{subset}}/N_{\text{total}}$; $N_{\text{subset}}/N_{\text{total}} \leq 0.1$).

It was suggested that the area under the curve for ROC plots (AUC) is used for reporting the enrichment results.⁶⁹ In addition, to characterize the “early” enrichment, enrichment percentages at 0.5%, 1%, 2%, and 5% of the docking database can be used. Here, we use a recently described measure that captures both aspects in one number, by using the logarithmic scale for the x-axis.⁷⁰

When multiple structures are available (either models or templates), a consensus enrichment was calculated by combining the docking results of multiple structures. For each docked compound, the best docking score across all structures was used for ranking the compound. Thus, the ranking relied on optimizing the protein conformation as well as protein–ligand complementarity.

Comparison of Ligand Enrichment. A difference in ligand enrichment values for two individual structures or models was defined to be significant if larger than 3 in the

logAUC units; otherwise, the enrichment values were considered to be comparable.

Statistical significance of the difference between the accuracies of two docking protocols was calculated by the following procedure. For each protocol, an enrichment value was calculated for each target in the benchmark set. The distribution of the protocol difference in enrichment values for each target was compared to the normal distribution using the Shapiro–Wilk test.⁷¹ If the difference was distributed normally at the confidence level of 95%, the dependent *t*-test for paired samples was performed to determine whether or not the differences between the two samples were statistically significant at this confidence level.⁷² Otherwise, the Wilcoxon signed-rank test was used.⁷³ These analyses were preformed using the statistical package R (<http://www.r-project.org>).

RESULTS

We begin by evaluating the comparative models in terms of their N-DOPE^{62,63} score and RMSD_{bs} from the holo X-ray structure of the target. For each of the 38 targets in the benchmark, the ability to identify known ligands is then compared for the holo X-ray structure, the apo X-ray structure, the individual comparative models, and their templates. Next, a consensus enrichment is calculated for each of the 38 targets by combining the docking scores against a variety of models (each based on a different template) and evaluated against enrichment values derived for single structures and models; a detailed analysis is performed for eight targets. Finally, we describe six examples of docking against a comparative model that reproduced the known binding geometry of the ligand.

Comparative Model Evaluation. Among the 222 templates used for model generation, 134 templates are holo X-ray structures, and 88 templates are apo X-ray structures. For both holo and apo templates, the number of structures decreases with an increase in the target–template sequence identity (Figure 1). In contrast, the sequence identity of the binding sites is distributed evenly, reflecting the relative conservation of the functional regions in evolution. The holo X-ray structures and comparative models of the 38 targets were assessed by the normalized DOPE score (N-DOPE). 34% of the models based on holo templates received N-DOPE scores below −1.0, 74% of the models received scores below 0.0, and 93% of the models received scores below 1.0. Nearly the same distribution of N-DOPE scores was found for models based on apo templates (33% below −1.0, 78% below 0.0, and 93% below 1.0). 49% of the models based on holo X-ray templates had RMSD_{bs} to their holo X-ray structure of less than 2.0 Å. A smaller fraction (33%) of the models based on apo templates showed the same deviation. Thus, we expect that the comparative models used here are representative of the whole range of comparative models likely to be used for ligand docking in real applications.

Ligand Enrichment for an Individual Model. The performance of comparative models in virtual ligand screening was evaluated by the percentage of area under the enrichment curve (logAUC) and compared to that from both the holo and the apo X-ray structures (Table 2). For 14 targets, the holo X-ray structure outperformed all comparative models; for nine targets, the enrichment of the holo X-ray

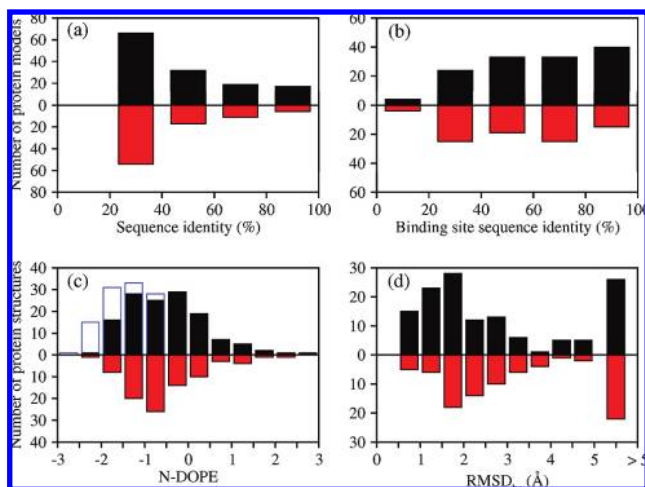


Figure 1. Composition of the benchmark. (a) Distribution of the target–template sequence identity for holo templates (black bars) and apo templates (red bars). (b) Distribution of the target–template binding site sequence identity. (c) Distribution of N-DOPE statistical potential score for comparative models (black and red bars for models based on holo and apo templates, respectively) and target X-ray structures (empty blue bars). (d) Distribution of root-mean-square deviation of the non-hydrogen atoms in binding site residues (RMSD_{bs}) between a comparative model and a target X-ray structure.

structure was comparable to that of the most enriching model; for the remaining 15 targets, the most enriching model outperformed the holo X-ray structure. Averaged over all 38 targets, the average logAUC for the holo X-ray structures is 30.6, which is only slightly higher than the average logAUC for the most enriching models (28.7). The difference between a holo X-ray structure and a most enriching model is not statistically significant. Considering the 34 targets for which both holo and apo X-ray structures were available, the average logAUC is 29.8 for the holo X-ray structures, 20.2 for the apo X-ray structures, and 28.7 for the most enriching models. For either the 38-target sample or the 34-target sample, the most enriching model tends to be significantly more enriching than the apo X-ray structure. We calculated binding site volumes for all models of the 38 targets.⁷⁴ There is no significant correlation between the enrichment and model binding site volume: The most enriching model has the largest/smallest volume of all target models in 7/6 out of the 38 cases.⁷⁵

These results suggest that the ability to identify the most enriching model of the target in the absence of knowing the actual ligands would be invaluable. Such an identification might be achieved by one or more predictors of model accuracy. Therefore, we asked whether there were model properties that might predict the most enriching model among multiple models based on different template structures. In fact, we found no good criterion for such a prediction. There is essentially no correlation between the ligand enrichment and template resolution ($R = -0.16$). The ligand enrichment is correlated only weakly with the accuracy of the binding site as measured by RMSD_{bs} ($R = -0.32$) (Figure 2), which is in any case unknown in the absence of the defined holo structure. We also calculated correlation coefficients between the ligand enrichment (logAUC) and three different properties of the model (Figure 2). There were only weak correlations of enrichment with the binding-site sequence identity ($R = 0.38$), the overall sequence identity ($R = 0.32$),

and the N-DOPE score ($R = -0.37$). For 38 targets, the average logAUC of the most enriching models was significantly higher than that of the models predicted to have the best enrichment using any of three criteria (average logAUC values were 21.0, 20.9, and 18.6 for the best-assessed models selected by binding-site sequence identity, the overall sequence identity, and the N-DOPE score, respectively). These criteria were thus unreliable predictors of docking success judged by ligand enrichment.

Ligand Enrichment for Multiple Models. Because the tested sequence and/or structural attributes were unreliable predictors of ligand enrichment, we turned to calculating enrichment using a “consensus” compound rank by combining multiple models, each based on a different template (Figure 3). For 11 and 7 of the 38 targets, the consensus enrichment for multiple models is respectively better and comparable to that for the holo X-ray structure. This compares to 15 and 9 for the most enriching model decided post hoc. For 16 and 8 of the 34 targets with an apo structure, the consensus enrichment is respectively better and comparable to that for apo structures; the average consensus enrichment is 23.6. The consensus enrichment is significantly better than the enrichment for the best-assessed model identified by the sequence identity. The difference between the consensus enrichment and the enrichment for the apo X-ray structure is not distinguishable at the 95% confidence level, but is statistically significant at the 85% confidence level. Consensus enrichment benefits from a de facto treatment of receptor flexibility through consideration of multiple target conformations, each one corresponding to a different comparative model based on a different template structure.

Two protocols further exploring the conformational space of the target were compared by their corresponding enrichments. In the first protocol, four new templates with sequence identities spanned by the original set of templates were added for each target; thus the number of models used for consensus enrichment calculations varied from 5 to 13 per target. In the second protocol, the original set of templates was used, but for each template the five models with the best MODELLER objective function values were used, not only the best scoring model; thus, the number of models used for consensus enrichment calculations was 5 times the number of templates, varying from 5 to 45.

These two protocols were tested on 10 of the original 38 targets (including six enzymes, two of which are kinases, and four hormone receptors) (Table 3). Using the first protocol, four targets yielded improved enrichment and six targets yielded enrichment comparable to that for the initial set of models; in no case did enrichment decrease. Using the second protocol, no clear trends were observed: one target yielded improved enrichment, two targets yielded worse enrichment, and seven targets yielded enrichment comparable to that for the initial set of models. Thus, it appears that ligand enrichment is better optimized by adding additional templates than by adding models based on the same template and with suboptimal values of the MODELLER objective function.

Docking to Templates Instead of Comparative Models. Comparative models rather than template structures are often used as targets for ligand screening. The comparative models and the corresponding template structures

Table 2. Ligand Enrichment Using X-ray Structures and Multiple Comparative Models^a

protein target	most enriching model		best model by sequence identity		consensus enrichment	holo X-ray enrichment	apo X-ray enrichment
	sequence identity [%]	enrichment	sequence identity [%]	enrichment			
ACE	44.1	50.2	54.8	37.9	48.9	40.6	44.1
ADA	26.5	40.3	84.8	38.8	41.1	22.7	46.3
COMT	20.1	0.0	20.1	0.0	0.0	27.6	1.9
PDE5	30.4	22.1	95.5	20.5	18.6	12.1	26.3
DHFR	27.9	34.6	37.3	13.1	20.3	18.9	67.2
GART	40.4	27.5	41.5	0.6	27.4	35.3	3.7
FXa	30.4	52.1	63.8	27.2	49.6	41.8	19.1
thrombin	30.0	43.4	39.5	36.9	42.4	29.4	56.2
trypsin	78.8	38.0	78.8	38.0	32.3	29.3	9.5
AChE	38.0	35.7	92.7	17.3	29.1	38.5	15.5
ALR2	68.7	41.9	86.6	39.5	37.1	39.7	24.6
AmpC	76.6	46.6	76.6	37.2	40.3	47.4	1.3
COX-1	63.4	26.2	63.4	26.2	25.3	28.3	24.1
COX-2	64.4	13.3	64.7	8.2	12.4	40.8	39.3
GPB	41.8	8.9	80.7	6.5	6.8	17.1	23.9
HIVPR	49.0	30.5	96.9	4.8	23.7	11.9	31.3
HIVRT	97.7	12.9	98.9	0.0	12.9	25.8	5.2
HMGR	100.0	43.2	100.0	43.2	41.5	40.9	44.7
InhA	29.0	14.6	29.0	14.6	11.8	8.2	10.1
NA	28.8	51.2	34.2	20.4	42.6	47.6	33.9
PARP	46.4	9.2	86.8	6.4	6.3	8.2	7.3
PNP	36.9	33.5	93.1	19.3	23.9	49.1	18.7
SAHH	84.7	82.4	84.7	82.4	78.4	82.8	20.3
CDK2	27.6	13.5	94.9	10.1	11.7	11.3	10.4
EGFr	37.7	13.2	38.1	12.3	10.7	21.5	16.0
FGFr1	41.3	12.3	51.0	6.2	11.9	6.7	4.9
HSP90	62.4	18.7	70.4	14.5	11.5	24.6	4.1
P38 MAP	29.4	31.4	62.2	21.2	15.6	12.5	10.4
SRC	68.8	13.8	82.0	13.4	12.3	9.5	10.3
TK	20.7	13.4	40.4	3.0	2.9	63.5	3.9
AR	56.0	31.7	84.3	31.5	14.5	48.2	
ER _{agonist}	93.1	41.0	93.1	41.0	19.6	55.4	40.3*
ER _{antagonist}	21.0	19.2	93.0	9.0	14.7	23.2	2.6
GR	27.4	18.8	56.6	15.2	16.7	20.5	
MR	56.8	30.5	56.8	30.5	29.5	57.0	
PPAR _g	20.2	13.2	65.0	9.2	8.8	4.4	11.3
PR	53.5	35.9	53.5	35.9	11.8	23.2	
RXR _α	87.0	26.9	88.8	2.0	11.2	37.9	0.0

^a Sequence identity, the sequence identity of the complete template and target sequences. Enrichment, the ligand enrichment is represented by logAUC. Consensus enrichment, logAUC calculated from docking scores against all target models. Holo X-ray enrichment, the enrichment for the holo X-ray structure of the target. The enrichment for the models is in bold when it is larger by 3 units than that for the holo X-ray structure. *, the ER apo structure used for both the ER agonist and the antagonist contains no ligands but adopts the conformation close to the ER agonist due to the binding of a glucocorticoid receptor-interacting protein 1 NR box II peptide.

determined by X-ray crystallography were compared by their ability to identify the known ligands (Table S1). To our surprise, no statistically distinguishable difference in ligand enrichment was found between the modeled structures and the templates, using either the most enriching model/template, the model/template with the highest sequence identity, or the consensus enrichment combining all models/templates. We examined the difference between the enrichments for each model–template pair ($\Delta\log\text{AUC}_{m-t} = \log\text{AUC}_{\text{model}} - \log\text{AUC}_{\text{template}}$). Among the 222 model–template pairs, models were better, comparable to, and worse than their templates for 30%, 39%, and 31% of the pairs, respectively.

$\Delta\log\text{AUC}_{m-t}$ is correlated weakly with the target–template sequence identity ($R_{\text{holo}} = 0.22$, $R_{\text{apo}} = 0.07$) (Figure 4a,b). Several models based on 20–40% sequence identity to their templates yielded much worse enrichments than their templates. A much stronger correlation was found between $\Delta\log\text{AUC}_{m-t}$ and the enrichment difference between the holo X-ray structure of the target and the template ($\Delta\log\text{AUC}_{x-t}$)

(Figure 4c,d). For both holo and apo model–template pairs, the correlation coefficients are above 0.5. In other words, the enrichment for a comparative model relative to its template is correlated with the enrichment for the target relative to its template. For instance, the target structure (PDB ID 3dfr) of dihydrofolate reductase (DHFR) from *Lactobacillus casei* yielded a ligand enrichment of 18.9. One template (PDB ID 1rc4), which is also a DHFR structure but from *Escherichia coli*, yielded an enrichment of 62.5. The comparative model based on this template showed an enrichment of 23.3, higher than that of the target structure. This result suggests that a template orthologous to the target may be more enriching than the target itself, whether the target structure is determined by X-ray crystallography or predicted by comparative modeling.

We hypothesized that comparative models achieve a better enrichment relative to the template structures when the target and template binding profiles are dissimilar. We obtained the corresponding subset of target–template pairs by eliminating orthologous pairs⁷² as well as nuclear hormone

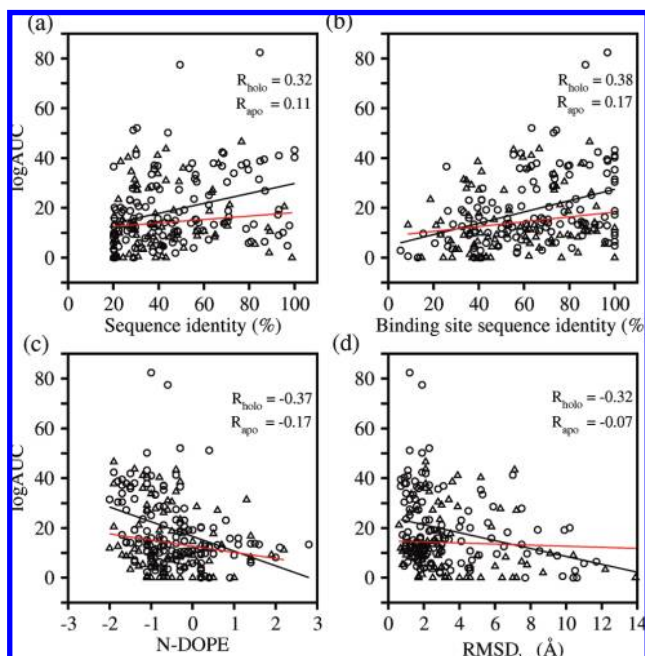


Figure 2. Model features do not predict docking success. “○” and “△” correspond to models built from holo- and apo-templates, respectively.

receptor pairs involving AR, GR, and MR that bind very similar ligands. For the remaining 124 paralogous target–template pairs, models were better, comparable to, and worse than their templates for 34%, 40%, and 26% of the pairs, respectively, in agreement with our hypothesis. Moreover, we also hypothesized that comparative models achieve a better enrichment relative to the template structures when comparative models are relatively accurate (i.e., the targets are not too different from the templates). Thus, we also removed from our benchmark the 37 target–template pairs with less than 25% sequence identity, leaving 39% of the original 222 target–template pairs. As a result, the models were better, comparable to, and worse than their templates for 42%, 41%, and 17% of the pairs, respectively, again in agreement with our hypothesis.

Detailed Analysis of Ligand Enrichment for Eight Targets. The enrichment for eight targets, including six enzymes and two hormone receptors, was examined in detail (Figure 5).

Adenosine deaminase (ADA) is a metalloenzyme, having a large binding pocket with a catalytic zinc ion coordinated by three histidine residues.^{76,77} Electrostatic interactions play an important role during ligand binding to this enzyme. The holo X-ray structure of the target is bound to a non-nucleoside inhibitor. Two other X-ray structures of adenosine deaminase were used as templates: one is an apo structure with 26% sequence identity to ADA; the other binds a purine nucleoside analogue and has 85% sequence identity to ADA. The enrichments (logAUC) for the two models were 40.3 and 38.8, much better than the logAUC of 22.7 for the holo X-ray structure (Table 2). Combining the docking results for both models, the consensus enrichment increased to 41.1. The poorer enrichment using the holo X-ray structure is not surprising in this case. Most known ligands of ADA are nucleoside analogues that form the major part of the ADA-like ligands in DUD. The target structure, binding to a relatively hydrophobic non-nucleoside inhibitor, undergoes

a conformational change that exposes hydrophobic patches. These patches may not be exposed when the target binds less hydrophobic ligands in DUD, rationalizing why the holo X-ray structure with a non-nucleoside inhibitor is less enriching than comparative models based on a more representative holo X-ray structure. In fact, the two templates also yielded better enrichment than did the target structure (28.9 and 31.5, respectively). This example illustrates the benefits of virtual screening with multiple models based on different templates.

Factor Xa (FXa) converts prothrombin to thrombin, which is the last enzyme in the coagulation cascade and is responsible for fibrin formation, platelet activation, and other physiological events.^{78,79} The binding site of FXa can accommodate structurally diverse inhibitors. In the holo X-ray structure, the inhibitor binds in an extended conformation through an ionic S1 pocket and a hydrophobic S4 pocket.⁸⁰ In the holo X-ray structure, the S2 pocket is blocked by Tyr99. Seven templates were used, with sequence identity to the target ranging from 24% to 64%. The model based on a holo template with 30% sequence identity yielded the highest enrichment 52.1, while the model based on an apo template with 24.0% sequence identity yielded the lowest enrichment 15.3. The consensus enrichment was 49.6, close to that achieved by the most-enriching model. The binding site in the most enriching model was similar to that in the holo X-ray structure. The S1 subsite mimicked the X-ray conformation and formed hydrogen bonds with most ligands through the anchor residues Asp189 and Gly219. The S4 subsite is lined by the aromatic rings of Phe174 and Tyr99 that are almost parallel with each other and perpendicular to the Trp215 ring. In the holo X-ray structure, these residues close down on the ligand and make the nearby subsite S2 inaccessible. In the most enriching model, the side chain of Tyr99 moved toward the outside of the S4 pocket and changed its χ_1 by 90°. The modeled S4 pocket thus became 14% larger in volume than that in the holo X-ray structure and presumably capable of binding a larger variety of ligands.⁷⁵ This hypothesis is supported by the improved enrichment relative to that for the holo X-ray structure. Thus, FXa provides another example of why multiple comparative models may be more useful for virtual screening than a single holo X-ray structure.

HIV protease (HIVPR) is a key enzyme for the production of infectious virus particles and is an important target for antiviral AIDS drugs. Numerous classes of substrate- and structure-based inhibitors have been designed, tested, and cocrystallized with the enzyme. The active site contains two extended β -hairpins (i.e., flaps) that sequester it from water and two catalytic aspartyl residues (Asp25 and Asp25') at the bottom of the ligand binding cavity.⁸¹ In the holo X-ray structure of the target, the protein binds a pentapeptide mimic in an extended conformation.⁸² This X-ray structure did not yield a high enrichment (11.9) because many other known ligands do not fit into this particular conformation. Twelve templates were found for HIVPR with a wide range of sequence identity from 23% to 97%. The highest enrichment, 30.5, was obtained from a model based on an apo template with 49% sequence identity. The improved enrichment for this model benefited from both the opening of the flaps that allowed most ligands to fit into the cavity, and the conservation of side-chain conformations at the bottom of the cavity,

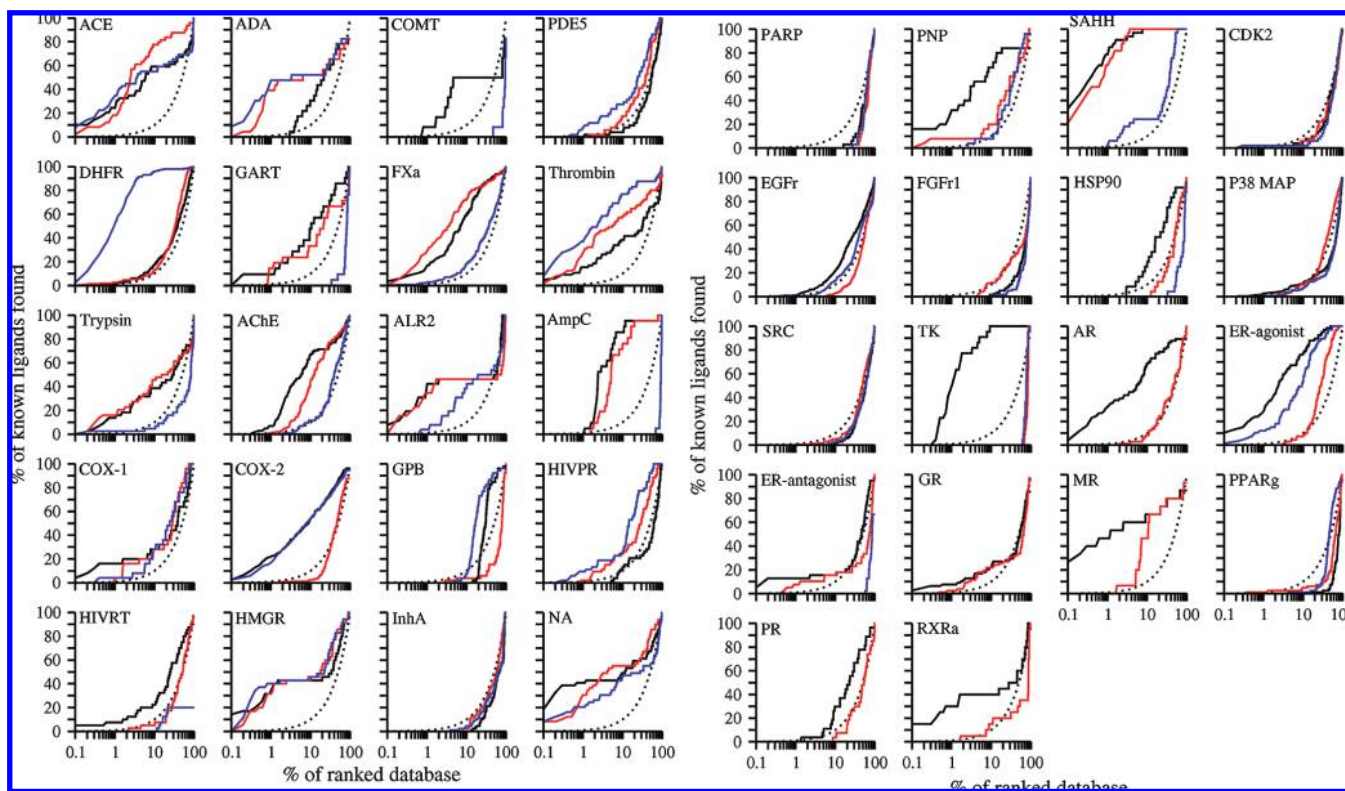


Figure 3. Enrichment plots for the 38 protein targets. Enrichment curves for the holo X-ray structure (black line), the apo X-ray structure (blue line), the consensus enrichment for multiple models (red line), and random selection (dotted line).

Table 3. Consensus Enrichment Using Additional Models^a

protein target	initial	addition of templates	addition of suboptimal models
COMT	0.0	10.2	0.0
GART	27.4	27.5	20.6
thrombin	42.4	55.8	47.1
GPB	6.8	6.9	6.2
EGFR	10.7	9.9	10.2
TK	2.9	2.5	3.0
AR	14.5	14.7	11.6
ER _{antagonist}	14.7	14.1	16.9
MR	29.5	43.9	21.0
PPARg	8.8	31.0	7.4

^a Initial, the consensus enrichment achieved by combining docking score for a set of models, each one of which is based on a different template (Table 2). Addition of templates, four templates were added to the initial set of templates. Addition of suboptimal models, the models with the top five MODELLER scores (not only the top model) were selected for each of the original templates.

including the two catalytic Asp residues. The consensus enrichment was 23.7, lower than that for the most enriching model but better than or comparable to the enrichments for all other models. The docking energies used to calculate the consensus enrichment were gathered from 11 models, among which six models contributed more than 10% of the scores of the known ligands each. This case again illustrates the advantages of using comparative models in different conformational states over a single holo X-ray structure.

Neuroaminidase (NA) is one of two glycoproteins expressed on the surface of the influenza virus and is responsible for the release of viruses from infected cells; the enzyme is the target for the anti-influenza drugs such as oseltamivir (Tamiflu) and zanamivir (Relenza), the latter of which was developed by structure-based design.⁸³ The holo

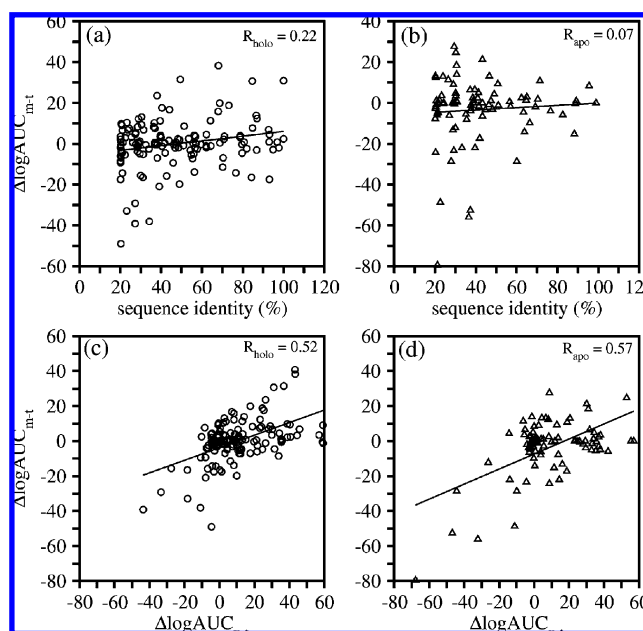


Figure 4. Comparing ligand enrichments for comparative models and their templates. “O” and “Δ” correspond to models based on holo- and apo-templates, respectively. (a,b) Scatter plots of the difference between the enrichments for a comparative model and the corresponding template ($\Delta\log\text{AUC}_{m-t} = \log\text{AUC}_{\text{model}} - \log\text{AUC}_{\text{template}}$) versus the target–template sequence identity. (c,d) Scatter plots of $\Delta\log\text{AUC}_{m-t}$ versus the difference between the enrichments for the target holo X-ray structure and the template ($\Delta\log\text{AUC}_{x-t} = \log\text{AUC}_{\text{X-ray}} - \log\text{AUC}_{\text{template}}$).

X-ray structure⁸⁴ showed a better enrichment for a small fraction of the ranked database than two models (Figure 5), with a logAUC of 47.6. One model based on a holo template with 29% sequence identity yielded the highest enrichment, 51.2. This modeled binding site was similar to that of the

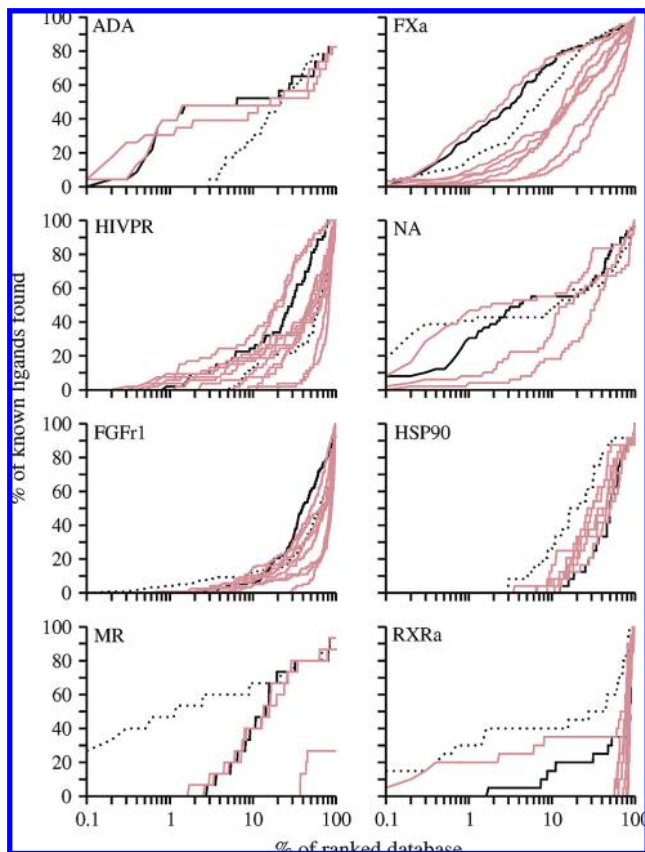


Figure 5. Sample enrichment curves. For eight targets (six enzymes, one of which is a kinase, and two hormone receptors), enrichment curves are plotted for the holo X-ray structure (dotted line), the consensus based on multiple models (black line), and each single model (brown lines).

holo X-ray structure. The consensus enrichment was 42.6, again close to that for the most enriching model.

Fibroblast growth factor receptor kinase (FGFR1) is a difficult target for virtual screening due to the receptor flexibility and the exposed binding site. Neither the holo X-ray structure in the DFG-in conformation nor the eight comparative models yielded enrichments above random. The highest enrichment was 12.3 from the model based on an apo template with 41% sequence identity. The consensus enrichment was 11.9, close to the highest enrichment observed for this target.

Heat shock protein 90 (HSP90) is an ATP binding protein responsible for stabilizing partially folded forms of many proteins. The holo X-ray structure yielded the enrichment for 24.6. Among the eight models built for this target, the model based on an apo template with 62% sequence identity achieved the highest enrichment for 18.7. However, two models, one based on a holo template with 20% sequence identity and the other one on an apo template with 43% sequence identity, failed because of the distortion of the binding site. The consensus enrichment was 11.5, worse than the enrichments for the other six models.

Mineralocorticoid receptor (MR) is a hormone receptor that integrates hormonal signaling and activates the expression of aldosterone target genes, which control several physiological processes including disorders of the nervous system, hypertension, and cardiac failure. The holo X-ray structure of the target binds aldosterone in a fully enclosed pocket. The A-ring ketone of aldosterone makes hydrogen

bonds with the side chains of Gln776 and Arg817. On the other side of the cavity, the hydroxyl and ketone groups in the C-ring and D-ring make hydrogen bonds with the side chains of Asn770 and Thr945.⁸⁵ The X-ray structure ligand is further pinned down by hydrophobic interactions with the binding site. The enrichment obtained using the holo X-ray structure is 57.0. Four models were generated on the basis of templates with sequence identities from 20% to 57%. Among them, the model based on the holo X-ray structure of progesterone receptor (PR) with 57% sequence identity yielded the best enrichment, 30.5. The consensus enrichment for multiple models is 29.5, close to the highest enrichment obtained. The PR structure used as the template for the most enriching model binds a nonsteroidal ligand tanaproget (TNPR).⁸⁶ In comparison to the aldosterone binding in the holo X-ray structure of the actual target, the 1-methyl-1*H*-pyrrole-2-carbonitrile ring of TNPR lies approximately between the A and B rings of aldosterone, while the 1,4-dihydro-3,1-benzoxazine-2-thione moiety lies close to the C and D rings of aldosterone. Like the A-ring ketone in aldosterone, the nitrile group of TNPR also hydrogen bonds with the main-chain amido groups of the Gln and Arg residues. The benzoxazine amide group at the distal end of TNPR forms hydrogen bonds with the Asn side chain. TNPR binds similarly as the aldosterone, forming hydrophobic contacts with the PR cavity. The geometry of hydrogen bonds and hydrophobic interactions in the most enriching model was similar to those in the holo X-ray structure with aldosterone. However, two differences were observed. First, the Arg817 side chain moved out of the modeled binding site because of the nitrile group in TNPR. Arg817 thus became less capable of forming hydrogen bonds with the A-ring ketone. Second, the Thr945 side chain in the target structure formed hydrogen bonds with the aldosterone, while the corresponding Thr in the PR template formed no hydrogen bonds with TNPR. Thus, Thr945 in the modeled binding site based on the PR template was incapable of hydrogen bonding with MR ligands. These two changes explain the decrease in the ligand enrichment obtained using the most enriching model relative to the holo X-ray structure.

Retinoic X receptor α (RXRa) is also a hormone receptor, mediating the biological effects of retinoids. RXRa uniquely forms heterodimers with other nuclear receptors, including peroxisome proliferator-activated receptor (PPAR). Furthermore, RXRa can heterodimerize in response to its ligands. Heterodimerization of RXRa can mediate diverse endocrine signaling pathways.⁸⁷ Hydrophobic interactions play an important role in the binding of the synthetic ligand BMS649 to the X-ray structure of the target. The carboxylate group of BMS649 also forms ionic interactions with the basic residue Arg316 and a hydrogen bond with the backbone amide of Ala327. Nine templates with a range of sequence identity from 20% to 89% were used to build comparative models. The enrichment obtained using the holo X-ray structure is 37.9. Among the nine models, only the model based on a holo template with 87% sequence identity yielded an enrichment above random (26.9). The consensus enrichment was 11.2, which is comparable to random selection. The decrease of ligand enrichment using the most enriching model relative to the holo X-ray structure is rationalized by a distortion of the anchor residue Arg316. In the holo X-ray structure of the target, both amines contributed to the ionic

interactions with BMS649. However, in the modeled binding site, the Arg316 side chain is rotated, so that only one guanidinium nitrogen points into the pocket. This rationalization is supported by the docking poses and energies of the known ligands, in comparison with BMS649. For instance, the known ligand Bexarotene docked into the modeled binding site similarly as in the holo X-ray structure, but received a less favorable docking energy due to a decrease in the electrostatic interaction energy.

Accuracy of the Docking Geometry in Modeled Binding Sites. Modeling and docking were evaluated primarily by their ability to identify known ligands among top-ranking docked molecules. We have not focused on predicting the conformation of each target in complex with its known ligands. Nevertheless, the predicted poses of a number of ligands turned out to be modeled relatively accurately, as illustrated by four enzymes and two hormone receptors (Figure 6).

In the target structure of DHFR, methotrexate binds to the large half-buried binding site with a neighboring cofactor NADP. A comparative model was generated using another DHFR structure as a template that shares 27% sequence identity to the target but only binds methotrexate without NADP. Aminoanfol, which contains the same diamino-pteridine and benzoic acid groups as methotrexate, was ranked 72 among DUD molecules (top 0.1%). The docked pose of aminoanfol accurately reproduced that of the cocrystallized methotrexate, resulting in an overlap of the equivalent diamino-pteridine and the benzoic acid groups. In the target structure of NA, zanamivir binds to the shallow and solvent-exposed binding site with essential hydrogen-bonding interactions. A comparative model was calculated on the basis of another neuraminidase structure with 29% sequence identity to the target and a bound sialic acid. In the modeled binding site, a carboxylic acid analogue, ranked 102 among DUD molecules, overlapped with the cocrystallized zanamivir on the guanidine, acetamido, and carboxylic acid groups (Figure 6b) and reproduced the hydrogen-bonding interactions in the target structure. The target structure of purine nucleoside phosphorylase (PNP) binds simultaneously immucillin H and an inorganic phosphate. A comparative model is generated using another PNP structure as a template that shares 37% sequence identity to the target and binds both an immucillin H analogue and a phosphate. The purine group of a ligand, ranked nine among DUD molecules, overlapped with the purine group of the immucillin H in the target. The target structure of *s*-adenosyl-homocysteine hydrolase (SAHH) binds an adenosine derivative and a neighboring cofactor NADP. A comparative model was calculated on the basis of another SAHH structure with 49% sequence identity to the target, a bound adenosine, and a neighboring cofactor NADP. In the modeled binding site, an adenosine derivative, ranked 15 among DUD molecules, overlapped with the adenosine in the target structure on both the adenine and the ribose rings. In the target structure of androgen receptor (AR), metribolone binds to the deeply buried binding site through hydrophobic interactions as well as hydrogen bonds using its ketone and hydroxyl groups. A comparative model was generated using another AR structure as a template that shares 70% sequence identity to the target and binds tetrahydrogestrinone. In the modeled binding site, metribolone, ranked 1167, accurately reproduced its binding

geometry in the target. In the target structure of retinoic X receptor α (RXRa), the ligand BMS649 binds to the L-shaped and elongated binding pocket through hydrophobic interactions⁸⁷ as well as a hydrogen bond using its carboxylate group. A comparative model was calculated on the basis of another RXR structure with 87% sequence identity to the target and a bound retinoic acid. Using this model, bexarotene, ranked 26 among DUD molecules, overlapped with the cocrystallized BMS649 on both the benzoic acid group and the tetramethylnaphthalene group.

Receptor-Based Matching Spheres. In this study, the docking protocol depends on the protein and ligand “matching spheres” to position small molecules in the binding site. Ideally, to reduce the size of the search space, the protein matching spheres should cover only the binding site surface and not other regions of the protein; similarly, the ligand matching spheres should cover only the space occupied by the ligands. For a holo X-ray structure, the matching spheres can be calculated in a straightforward manner from the knowledge of the protein–ligand complex coordinates (Methods), although even in that case they may under- or overestimate the available protein and ligand volumes for other ligands. For the apo X-ray structures and comparative models, exactly the same matching spheres were used in our benchmark. This computation may have introduced a bias in our results; in realistic applications, the holo X-ray structure will often not be available. In principle, this bias could be either positive or negative. For example, using the “holo X-ray” matching spheres can productively restrict the sampling space as compared to a looser definition of the binding site and lead to a reasonable enrichment (e.g., the most enriching model of HIVPR); alternatively, restricting the sampling too much on the basis of a small ligand in the holo X-ray structure may hurt identifying larger ligands (e.g., using the receptor-based spheres, the most enriching thrombin model yielded enrichment better than that using the “holo X-ray” matching spheres).

We investigated a potential benchmarking bias resulting from using “holo X-ray” matching spheres for docking against apo structures and models. For each of the 38 targets, 35 “binding site” matching spheres were generated independently for each structure (the holo X-ray structure, the apo X-ray structure, and each of the comparative models), based on the binding site residues identified in the holo X-ray structure (in many real applications, this information would have to be obtained from some other source); the ligand matching spheres were not used to restrict the sampling of the ligand position and conformation. On average, the best enrichment and consensus enrichment decrease by 10% (3 units) and 16% (4 units), respectively, when using “binding site” matching spheres instead of “holo X-ray” matching spheres (Table S2), presumably due to omitting ligand matching spheres. However, the order of enrichment for different types of structures and models remains unchanged, thus supporting our benchmarking.

DISCUSSION

Overview. Three key results emerge from this study. First, if multiple models based on different templates are used, one can frequently find at least one model that outperforms even the holo X-ray structure of the target. This encouraging

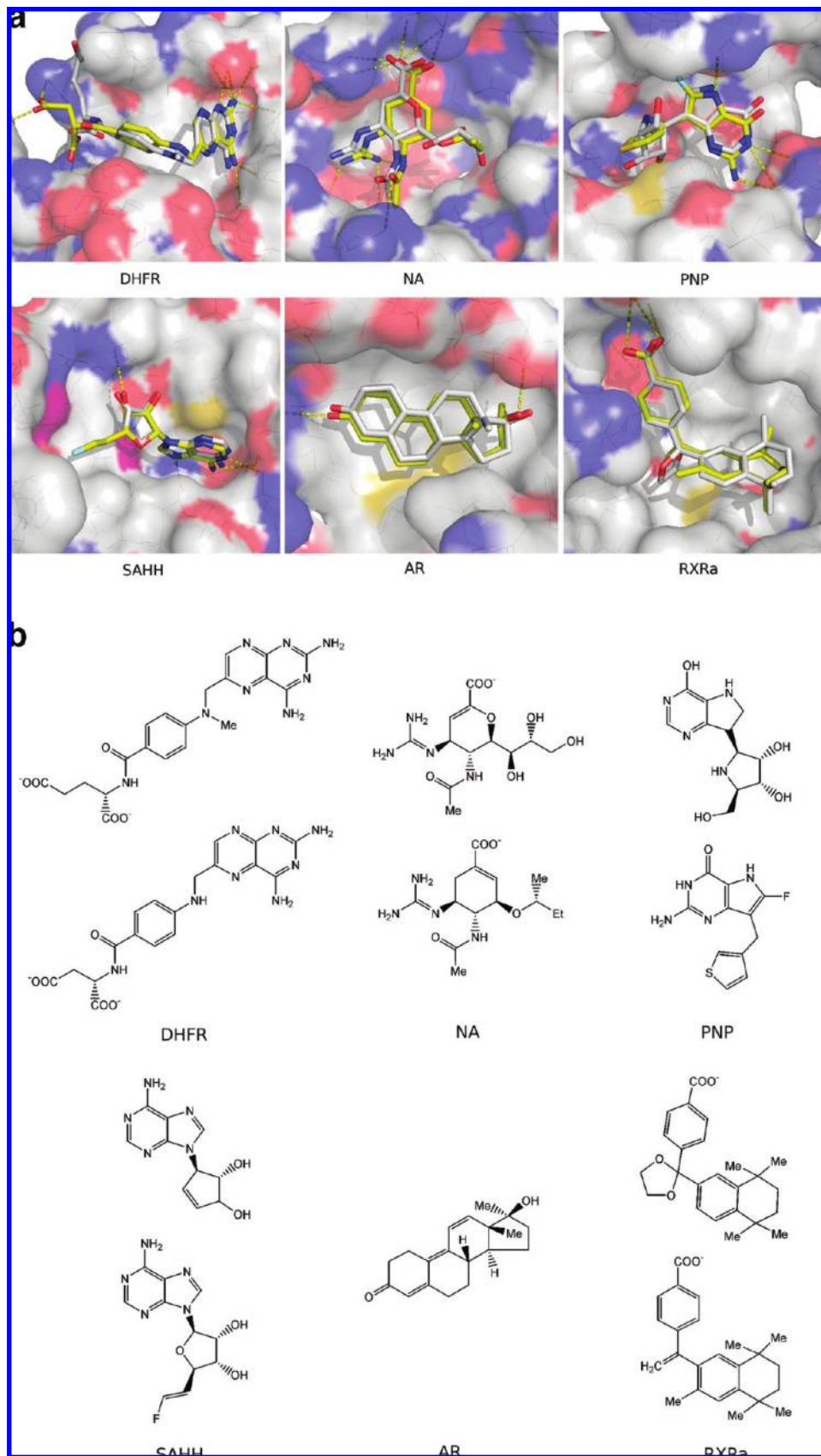


Figure 6. (a) Binding poses of six protein targets. For each target, the docking pose of one known binder with one comparative model of the target was selected. The ligand in complex with the crystallographic structure of the target protein was always located in the background. The targets include two hormone receptors AR and RXRa, and four enzymes DHFR, NA, PNP, and SAHH. (b) 2D images of ligands in Figure 6a. The ligands used in Figure 6a are presented. For AR, the ligands crystallized in the structures of target proteins are the same as the docked ligands. For the other five targets, the X-ray structure ligands are shown on top of the docked ligands.

result is mitigated by our inability to predict the optimal model for ligand enrichment in the absence of knowing the actual ligands; the enrichment shows little relationship to standard metrics of model attributes such as sequence identity or protein-structure-based scores.

Second, we find that over the DUD set the template structures typically perform as well as the comparative models that are built from them. This result is dispiriting at a first glance, suggesting that models having the correct sequence are not better targets than the template experimental structures from which they are built. However, it is 2.5 times as likely that a model is more enriching than the corresponding template, when the target and template binding profiles are dissimilar (i.e., the target and template are not orthologues) and when comparative models are relatively accurate (i.e., they are based on more than 25% sequence identity).

These first two observations lead to a final point: If models built on the basis of different templates are considered, the corresponding consensus enrichment frequently outperforms the enrichment yielded by the apo X-ray structure of the same target. Whereas these consensus enrichments still tend to be outperformed by the enrichments yielded by the holo X-ray structures, they are often competitive with them. We consider each of these points in turn.

Models versus Target Structure. We assessed the utility of comparative models in virtual ligand screening, through comparison with the holo and apo X-ray structures. The results showed that docking against comparative models frequently substantially enriches known ligands (Table 2). For 15 targets, the most enriching model is better for virtual screening than the holo X-ray structure; for nine targets, the most enriching model is as good as the holo X-ray structure. Twenty-seven most enriching models and 29 holo X-ray structures yielded better ligand enrichment than random selection. This result suggests that the conformational space spanned by multiple comparative models, each based on a different template, will overlap to some degree with an ensemble of conformations for the receptor in complex with different ligands. However, we could not find any features of comparative models or templates that reliably predict the most enriching model (Figure 2). This result is consistent with two earlier studies^{39,55} and can be rationalized as follows. The docking library contains multiple ligands for proteins in the target family. These ligands may have different affinities for different receptor conformations. One comparative model may yield a better enrichment than another model based on a more similar template sequence but lesser binding affinity for the target ligands.

Model versus Template Structure. Our results are consistent with the observation on a smaller benchmark that docking to a comparative model is on average as successful as docking to its template.⁵⁵ In fact, for our benchmark as a whole, we found that it is approximately equally likely a model will be more enriching, comparable to, or less enriching than a template (Table S1, Figure 4). There are two explanations for this observation.

First, many target–template pairs are orthologous (i.e., belonging to the same family and thus having very similar ligand binding profiles). In such cases, there is no reason to expect templates would on average result in a lower enrichment for the target ligands than a target model or even the target X-ray structure (Figure 4c,d). For example, in the

case of dihydrofolate reductase (DHFR), models were built on the basis of eight templates that are orthologous DHFRs from different species. Six of these eight templates yielded better ligand enrichments than the target structure, and four out of the six templates resulted in comparative models that yielded an enrichment better than or comparable to that of the holo X-ray structure. As expected, when the orthologous template–target pairs are excluded, comparative models enrich the ligands slightly better than the templates.

Second, models and templates also result in comparable (low) enrichment when both the template and the model are an inaccurate representation of the target holo structure. Such a situation tends to arise when the target–template sequence similarity is low (i.e., less than 25% sequence identity). As a special case, errors in the modeling of induced fit can explain why the holo models are more likely than the apo models to be more enriching than their templates (Figure 4a,b). When the 37 target–template pairs with less than 25% sequence identity are removed from the 124 paralogous target–template pairs (out of the 222 pairs in our benchmark), the enrichment obtained for models was better than, comparable to, and worse than that of their templates for 42%, 41%, and 17% of the pairs, respectively.

Consensus Enrichment. Most proteins are flexible, adopting different conformations when binding to different ligands. Thus, methods that can handle this variability are needed.^{10,11,88–92} The receptor variability has been considered during docking by using a “soft” representation of the receptor,^{93–95} minimizing the scoring function with respect to side-chain orientations,^{96–102} and allowing protein flexibility via molecular dynamics (MD) and Monte Carlo (MC) simulations.^{103–116} The receptor variability has also been partly addressed by docking to an ensemble of static receptor conformations. This ensemble can be derived experimentally by X-ray crystallography or NMR spectroscopy,^{117–123} alternatively, the ensemble can be derived computationally by MD/MC simulations,^{124–130} normal-mode analysis,¹³¹ or protein structure prediction.^{132,133} In this study, multiple comparative models were built for the target sequence, each based on a different template structure. We now turn to calculating a “consensus” enrichment on the basis of multiple models and/or templates, motivated by the observations that the most enriching of the multiple models frequently yields a better enrichment than the holo X-ray structure of the target and that no model/template feature can accurately predict the most enriching model.

Overall, the consensus enrichment outperformed the enrichments for both the apo X-ray structures and the best-assessed models (by sequence identity or the N-DOPE score). For 11/7 and 16/8 targets, the consensus enrichment is better than or comparable to the enrichment obtained using the holo and the apo X-ray structures, respectively (Figure 3). For 23 targets, the consensus enrichment was better than random selection. Consensus enrichment benefits from maximizing the number of binding modes presented by different template structures (Table 3). This interpretation is supported by examples, such as phosphodiesterase 5 (PDE5), DHFR, and thrombin. For these targets, the consensus scores of top-ranked ligands were contributed by docking screens against different comparative models, although we did not find a clear difference in the chemotypes of the top-ranked ligands preferred by different models. The combination of individual

docking screens against different models can frequently rescue ligands that are missed in a docking screen to a single inaccurate model.

Consensus enrichment was also calculated for each target–template pair, combining the docking results of a single model and the corresponding template (data not shown). For the 222 target–template pairs, the consensus enrichment was better than, comparable to, and worse than the enrichment for 23% (23%), 72% (67%), and 5% (10%) of the models (templates), respectively. When orthologous target–template pairs,⁷² hormone receptor pairs involving AR, GR, and MR, and pairs with less than 25% sequence identity were removed, further improvement of the consensus enrichment over the template-based enrichment was observed. For the 87 target–template pairs, the consensus enrichment was better and worse than the template enrichment in 33% and 3% of the cases, respectively. Thus, it is 11 times as likely that a model–template pair is more enriching than the template alone, when the target and the template are not orthologues and the model is based on a template with more than 25% sequence identity to the target.

Consensus enrichment of multiple templates was also shown to be better than that of a single, best-assessed template (Table S1), suggesting that the consensus enrichment can be used in docking screens where multiple experimentally determined structures are available. Furthermore, when the docking results of all models and templates were combined, the resulting consensus enrichment is frequently better than (29%) or comparable to (47%) the higher of the values for the consensus enrichment of all models and the consensus enrichment of all templates.

In summary, applications, such as protein function prediction or ligand discovery, could benefit from the consensus enrichment that combines docking screens against multiple experimentally determined structures of the protein target, multiple comparative models, and the templates on which these models are based.

Several “consensus” scoring methods have been suggested.¹³⁴ In distinction to our approach, however, these methods use multiple scoring functions, not multiple comparative models based on different templates. In principle, both types of consensus scoring could be combined with each other.

CONCLUSIONS

We conclude by returning to the questions we asked in the Introduction, for the modeling, docking, and benchmark. As for all quantifications of enrichment differences, a difference in logAUC of 3 units or more is considered significant.

How Does Docking against Comparative Models Compare to Random Selection? Comparative models typically outperform random selection significantly, doing so for 27 out of the 38 targets (Table 2).

How Does Docking against Comparative Models Compare to Docking against the Template Structures? For the entire benchmark, comparative models are on average no more enriching than the corresponding templates. This measurement, however, is confounded by the likelihood of orthologous templates genuinely recognizing the ligands for the modeled target. Conversely, a modeled structure based

on a paralogous template with at least 25% sequence identity to the target is 2.5 times more likely to be significantly more enriching than the template (see Docking to Templates Instead of Comparative Models section in Results).

If Multiple Models Are Calculated for a Target, Each One Based on a Different Template, Can Any of Them Outperform Apo and Even Holo X-ray Structures of the Target? Typically, the holo X-ray structure returns the best enrichments, but the modeled structures are often competitive. For 15 of the 38 targets, the most enriching model is better for virtual screening than the holo X-ray structure; for nine targets, the most enriching model is as good as the holo X-ray structure (Table 2). As compared to apo X-ray structures, the model performance is better still.

Can One Reliably Identify Which Model Will Be Most Enriching? No, none of the tested sequence or structural attributes (i.e., the overall target–template sequence identity, the binding site target–template sequence identity, and the predicted accuracy of a model) can reliably predict the accuracy of ligand docking (Table 2, Figure 2).

Can the Docking Screens Be Improved by Employing Multiple Models Instead of a Single Model? Yes. For the 38 targets, the enrichment of the model based on the highest sequence identity is better than or comparable to the enrichment for the apo and holo X-ray structures in 65% and 45% cases, respectively (Table 2); in contrast, the consensus enrichment for multiple models (and templates) is better than or comparable to the enrichment for the apo and holo X-ray structures in 70% (79%) and 47% (50%) cases, respectively (Table 2, Table S1). For the 222 target–template pairs, the consensus enrichment is better and worse than the template enrichment in 23% and 10% of the cases, respectively. For the 87 paralogous target–template pairs related at more than 25% sequence identity, the consensus enrichment is better and worse than the template enrichment in 33% and 3% of the cases, respectively (see Consensus Enrichment section in Discussion).

In conclusion, these results suggest techniques to best exploit comparative models in molecular docking screens: Whether one or multiple templates are available, comparative models are best used via consensus enrichment calculations that include multiple models as well as templates. For a single template, however, the corresponding comparative model tends to be more enriching than the template only if the template is paralogous and shares more than 25% sequence identity with the target.

ACKNOWLEDGMENT

We thank Dr. Niu Huang for discussions about the DUD database and the automated docking pipeline. We thank Dr. Peter Kolb for discussion about the manuscript. We acknowledge funds from the Sandler Family Supporting Foundation and National Institutes of Health (P01 GM71790 and R01 GM54762 to Dr. Andrej Sali and R01 GM59957 to Dr. Brian Shoichet). We are also grateful to Ron Conway, Mike Homer, Hewlett-Packard, IBM, NetApp, and Intel for hardware gifts.

Supporting Information Available: Ligand enrichments obtained by docking against the template structures, ligand

enrichments using the receptor-based matching spheres, and source organisms of all 38 targets and 222 templates. This material is available free of charge via the Internet at <http://pubs.acs.org>.

REFERENCES AND NOTES

- Kuntz, I. D. Structure-based strategies for drug design and discovery. *Science* **1992**, 257, 1078–1082.
- Klebe, G. Recent developments in structure-based drug design. *J. Mol. Med.* **2000**, 78, 269–281.
- Dailey, M. M.; Hait, C.; Holt, P. A.; Maguire, J. M.; Meier, J. B.; Miller, M. C.; Petraccone, L.; Trent, J. O. Structure-based drug design: From nucleic acid to membrane protein targets. *Exp. Mol. Pathol.* **2009**, 86, 141–150.
- Ealick, S. E.; Armstrong, S. R. Pharmacologically relevant proteins. *Curr. Opin. Struct. Biol.* **1993**, 3, 861–867.
- Gschwend, D. A.; Good, A. C.; Kuntz, I. D. Molecular docking towards drug discovery. *J. Mol. Recognit.* **1996**, 9, 175–186.
- Hoffmann, D.; Kramer, B.; Washio, T.; Steinmetzer, T.; Rarey, M.; Lengauer, T. Two-stage method for protein-ligand docking. *J. Med. Chem.* **1999**, 42, 4422–4433.
- Stahl, M.; Rarey, M. Detailed analysis of scoring functions for virtual screening. *J. Med. Chem.* **2001**, 44, 1035–1042.
- Charifson, P. S.; Corkery, J. J.; Murcko, M. A.; Walters, W. P. Consensus scoring: A method for obtaining improved hit rates from docking databases of three-dimensional structures into proteins. *J. Med. Chem.* **1999**, 42, 5100–5109.
- Abagyan, R.; Totrov, M. High-throughput docking for lead generation. *Curr. Opin. Chem. Biol.* **2001**, 5, 375–382.
- Klebe, G. Virtual ligand screening: strategies, perspectives and limitations. *Drug Discovery Today* **2006**, 11, 580–594.
- Sperandio, O.; Miteva, M. A.; Delfaud, F.; Villoutreix, B. O. Receptor-based computational screening of compound databases: The main docking-scoring engines. *Curr. Protein Pept. Sci.* **2006**, 7, 369–393.
- Berman, H. M.; Westbrook, J.; Feng, Z.; Gilliland, G.; Bhat, T. N.; Weissig, H.; Shindyalov, I. N.; Bourne, P. E. The protein data bank. *Nucleic Acids Res.* **2000**, 28, 235–242.
- Bairoch, A.; Bougueleret, L.; Altairac, S.; Amendolia, V.; Auchincloss, A.; Puy, G. A.; Axelsen, K.; Baratin, D.; Blatter, M. C.; Boeckmann, B.; Bollondi, L.; Boutet, E.; Quintaje, S. B.; Breuza, L.; Bridge, A.; Saux, V. B. L.; deCastro, E.; Ciampina, L.; Coral, D.; Coudert, E.; Cusin, I.; David, F.; Delbard, G.; Dornevil, D.; Duek-Roggli, P.; Duvaud, S.; Estreicher, A.; Famiglietti, L.; Farriol-Mathis, N.; Ferro, S.; Feuermann, M.; Gasteiger, E.; Gateau, A.; Gehant, S.; Gerritsen, V.; Gos, A.; Gruaz-Gumowski, N.; Hinz, U.; Hulo, C.; Hulo, N.; Innocenti, A.; James, J.; Jain, E.; Jimenez, S.; Jungo, F.; Junker, V.; Keller, G.; Lachaize, C.; Lane-Guermonprez, L.; Langendijk-Genevaux, P.; Lara, V.; Le Mercier, P.; Lieberherr, D.; Lima, T. D.; Mangold, V.; Martin, X.; Michoud, K.; Moinat, M.; Morgat, A.; Nicolas, M.; Paesano, S.; Pedruzzi, I.; Perret, D.; Phan, I.; Pilboud, S.; Pillet, V.; Poux, S.; Pozzato, M.; Redaschi, N.; Reynaud, S.; Rivoire, C.; Roechert, B.; Sapsezian, C.; Schneider, M.; Sigrist, C.; Sonesson, K.; Staehli, S.; Stutz, A.; Sundaram, S.; Tognolli, M.; Verbregue, L.; Veuthey, A. L.; Vitarello, C.; Yip, L.; Zuletta, L. F.; Apweiler, R.; Alam-Faruchy, Y.; Barrell, D.; Bower, L.; Browne, P.; Chan, W. M.; Daugherty, L.; Donate, E. S.; Eberhardt, R.; Fedotov, A.; Foulger, R.; Frigerio, G.; Garavelli, J.; Golin, R.; Horne, A.; Jacobsen, J.; Kleen, M.; Kersey, P.; Laiho, K.; Legge, D.; Magrane, M.; Martin, M. J.; Monteiro, P.; O'Donovan, C.; Orchard, S.; O'Rourke, J.; Patient, S.; Pruess, M.; Sitnov, A.; Whitefield, E.; Wieser, D.; Lin, Q.; Rynbeek, M.; di Martino, G.; Donnelly, M.; van Rensburg, P.; Wu, C.; Arighi, C.; Arminski, L.; Barker, W.; Chen, Y. X.; Crooks, D.; Hu, Z. Z.; Hua, H. K.; Huang, H. Z.; Kahsay, R.; Mazumder, R.; McGarvey, P.; Natale, D.; Nikolskaya, A. N.; Petrova, N.; Suzek, B.; Vasudevan, S.; Vinayaka, C. R.; Yeh, L. S.; Zhang, J.; Consortium, U. The universal protein resource (UniProt). *Nucleic Acids Res.* **2008**, 36, D190–D195.
- Pieper, U.; Eswar, N.; Webb, B.; Eramian, E.; Kelly, L.; Barkan, D. T.; Carter, H.; Mankoo, P.; Karchin, R.; Marti-Renom, M. A.; Davis, F. P.; Sali, A.; Sanchez, R. MODBASE, a database of annotated comparative protein structure models, and associated resources. *Nucleic Acids Res.* **2009**, 37, D347–D354.
- Baker, D.; Sali, A. Protein structure prediction and structural genomics. *Science* **2001**, 294, 93–96.
- Baker, D. A surprising simplicity to protein folding. *Nature* **2000**, 405, 39–42.
- Bonneau, R.; Baker, D. Ab initio protein structure prediction: Progress and prospects. *Annu. Rev. Biophys. Biomol. Struct.* **2001**, 30, 173–189.
- Marti-Renom, M. A.; Stuart, A. C.; Fiser, A.; Sanchez, R.; Melo, F.; Sali, A. Comparative protein structure modeling of genes and genomes. *Annu. Rev. Biophys. Biomol. Struct.* **2000**, 29, 291–325.
- Sali, A. 100,000 protein structures for the biologist. *Nat. Struct. Biol.* **1998**, 5, 1029–1032.
- Chandonia, J. M.; Brenner, S. E. The impact of structural genomics: Expectations and outcomes. *Science* **2006**, 311, 347–351.
- Liu, J. F.; Montelione, G. T.; Rost, B. Novel leverage of structural genomics. *Nat. Biotechnol.* **2007**, 25, 850–853.
- Jacobson, M.; Sali, A. Comparative protein structure modeling and its applications to drug discovery. *Annu. Rep. Med. Chem.* **2004**, 39, 259–276.
- Bissantz, C.; Bernard, P.; Hibert, M.; Rognan, D. Protein-based virtual screening of chemical databases. II. Are homology models of G-protein coupled receptors suitable targets? *Proteins: Struct., Funct., Genet.* **2003**, 50, 5–25.
- Cavasotto, C. N.; Orry, A. J. W.; Abagyan, R. A. Structure-based identification of binding sites, native ligands and potential inhibitors for G-protein coupled receptors. *Proteins: Struct., Funct., Genet.* **2003**, 51, 423–433.
- Evers, A.; Klebe, G. Ligand-supported homology modeling of G-protein-coupled receptor sites: Models sufficient for successful virtual screening. *Angew. Chem., Int. Ed.* **2004**, 43, 248–251.
- Evers, A.; Klebe, G. Successful virtual screening for a submicromolar antagonist of the neurokinin-1 receptor based on a ligand-supported homology model. *J. Med. Chem.* **2004**, 47, 5381–5392.
- Evers, A.; Klabunde, T. Structure-based drug discovery using GPCR homology modeling: Successful virtual screening for antagonists of the Alpha1A adrenergic receptor. *J. Med. Chem.* **2005**, 48, 1088–1097.
- Moro, S.; Deflorian, F.; Bacilieri, M.; Spalluto, G. Novel strategies for the design of new potent and selective human A(3) receptor antagonists: An update. *Curr. Med. Chem.* **2006**, 13, 639–645.
- Nowak, M.; Kolaczowski, M.; Pawlowski, M.; Bojarski, A. J. Homology modeling of the serotonin 5-HT1A receptor using automated docking of bioactive compounds with defined geometry. *J. Med. Chem.* **2006**, 49, 205–214.
- Chen, J. Z.; Wang, J. M.; Xie, X. Q. GPCR structure-based virtual screening approach for CB2 antagonist search. *J. Chem. Inf. Model.* **2007**, 47, 1626–1637.
- Zylberg, J.; Ecke, D.; Fischer, B.; Reiser, G. Structure and ligand-binding site characteristics of the human P2Y(11) nucleotide receptor deduced from computational modelling and mutational analysis. *Biochem. J.* **2007**, 405, 277–286.
- Radestock, S.; Weil, T.; Renner, S. Homology model-based virtual screening for GPCR ligands using docking and target-biased scoring. *J. Chem. Inf. Model.* **2008**, 48, 1104–1117.
- Singh, N.; Cheve, G.; Ferguson, D. M.; McCurdy, C. R. A combined ligand-based and target-based drug design approach for G-protein coupled receptors: application to salvinorin A, a selective kappa opioid receptor agonist. *J. Comput.-Aided Mol. Des.* **2006**, 20, 471–493.
- Kiss, R.; Kiss, B.; Konczol, A.; Szalai, F.; Jelinek, I.; Laszlo, V.; Noszal, B.; Falus, A.; Keseru, G. M. Discovery of novel human histamine H4 receptor ligands by large-scale structure-based virtual screening. *J. Med. Chem.* **2008**, 51, 3145–3153.
- de Graaf, C.; Foata, N.; Engkvist, O.; Rognan, D. Molecular modeling of the second extracellular loop of G-protein coupled receptors and its implication on structure-based virtual screening. *Proteins: Struct., Funct., Bioinform.* **2008**, 71, 599–620.
- Diller, D. J.; Li, R. X. Kinases, homology models, and high throughput docking. *J. Med. Chem.* **2003**, 46, 4638–4647.
- Oshiro, C.; Bradley, E. K.; Eksterowicz, J.; Evensen, E.; Lamb, M. L.; Lanctot, J. K.; Putta, S.; Stanton, R.; Grootenhuis, P. D. J. Performance of 3D-database molecular docking studies into homology models. *J. Med. Chem.* **2004**, 47, 764–767.
- Nguyen, T. L.; Gussio, R.; Smith, J. A.; Lannigan, D. A.; Hecht, S. M.; Scudiero, D. A.; Shoemaker, R. H.; Zaharevitz, D. W. Homology model of RSK2 N-terminal kinase domain, structure-based identification of novel RSK2 inhibitors, and preliminary common pharmacophore. *Bioorg. Med. Chem.* **2006**, 14, 6097–6105.
- Rockey, W. M.; Elcock, A. H. Structure selection for protein kinase docking and virtual screening: Homology models or crystal structures. *Curr. Protein Pept. Sci.* **2006**, 7, 437–457.
- Schapira, M.; Abagyan, R.; Totrov, M. Nuclear hormone receptor targeted virtual screening. *J. Med. Chem.* **2003**, 46, 3045–3059.
- Marhefka, C. A.; Moore, B. M.; Bishop, T. C.; Kirkovsky, L.; Mukherjee, A.; Dalton, J. T.; Miller, D. D. Homology modeling using multiple molecular dynamics simulations and docking studies of the human androgen receptor ligand binding domain bound to testosterone and nonsteroidal ligands. *J. Med. Chem.* **2001**, 44, 1729–1740.
- Kasuya, A.; Sawada, Y.; Tsukamoto, Y.; Tanaka, K.; Toya, T.; Yanagi, M. Binding mode of ecdysone agonists to the receptor:

- comparative modeling and docking studies. *J. Mol. Model.* **2003**, *9*, 58–65.
- (43) Li, R. S.; Chen, X. W.; Gong, B. Q.; Selzer, P. M.; Li, Z.; Davidson, E.; Kurzban, G.; Miller, R. E.; Nuzum, E. O.; McKerrow, J. H.; Fletcher, R. J.; Gilmor, S. A.; Craik, C. S.; Kuntz, I. D.; Cohen, F. E.; Kenyon, G. L. Structure-based design of parasitic protease inhibitors. *Bioorg. Med. Chem.* **1996**, *4*, 1421–1427.
- (44) Selzer, P. M.; Chen, X. W.; Chan, V. J.; Cheng, M. S.; Kenyon, G. L.; Kuntz, I. D.; Sakanari, J. A.; Cohen, F. E.; McKerrow, J. H. Leishmania major: Molecular modeling of cysteine proteases and prediction of new nonpeptide inhibitors. *Exp. Parasitol.* **1997**, *87*, 212–221.
- (45) Enyedy, I. J.; Ling, Y.; Nacro, K.; Tomita, Y.; Wu, X. H.; Cao, Y. Y.; Guo, R. B.; Li, B. H.; Zhu, X. F.; Huang, Y.; Long, Y. Q.; Roller, P. P.; Yang, D. J.; Wang, S. M. Discovery of small-molecule inhibitors of bcl-2 through structure-based computer screening. *J. Med. Chem.* **2001**, *44*, 4313–4324.
- (46) de Graaf, C.; Oostenbrink, C.; Keizers, P. H. J.; van der Wijst, T.; Jongejan, A.; Vemleulen, N. P. E. Catalytic site prediction and virtual screening of cytochrome P450 2D6 substrates by consideration of water and rescoring in automated docking. *J. Med. Chem.* **2006**, *49*, 2417–2430.
- (47) Katritch, V.; Byrd, C. M.; Tseitlin, V.; Dai, D. C.; Raush, E.; Totrov, M.; Abagyan, R.; Jordan, R.; Hruby, D. E. Discovery of small molecule inhibitors of ubiquitin-like poxvirus proteinase 17L using homology modeling and covalent docking approaches. *J. Comput.-Aided Mol. Des.* **2007**, *21*, 549–558.
- (48) Mukherjee, P.; Desai, P. V.; Srivastava, A.; Tekwani, B. L.; Avery, M. A. Probing the structures of leishmanial farnesyl pyrophosphate synthases: Homology modeling and docking studies. *J. Chem. Inf. Model.* **2008**, *48*, 1026–1040.
- (49) Song, L.; Kalyanaraman, C.; Fedorov, A. A.; Fedorov, E. V.; Glasner, M. E.; Brown, S.; Imker, H. J.; Babbitt, P. C.; Almo, S. C.; Jacobson, M. P.; Gerlt, J. A. Prediction and assignment of function for a divergent N-succinyl amino acid racemase. *Nat. Chem. Biol.* **2007**, *3*, 486–491.
- (50) Kalyanaraman, C.; Imker, H. J.; Federov, A. A.; Federov, E. V.; Glasner, M. E.; Babbitt, P. C.; Almo, S. C.; Gerlt, J. A.; Jacobson, M. P. Discovery of a dipeptide epimerase enzymatic function guided by homology modeling and virtual screening. *Structure* **2008**, *16*, 1668–1677.
- (51) Rotkiewicz, P.; Sicinska, W.; Kolinski, A.; DeLuca, H. F. Model of three-dimensional structure of vitamin D receptor and its binding mechanism with 1 α ,25-dihydroxyvitamin D-3. *Proteins: Struct., Funct., Genet.* **2001**, *44*, 188–199.
- (52) Que, X. C.; Brinen, L. S.; Perkins, P.; Herdman, S.; Hirata, K.; Torian, B. E.; Rubin, H.; McKerrow, J. H.; Reed, S. L. Cysteine proteinases from distinct cellular compartments are recruited to phagocytic vesicles by Entamoeba histolytica. *Mol. Biochem. Parasitol.* **2002**, *119*, 23–32.
- (53) Parrill, A. L.; Echols, U.; Nguyen, T.; Pham, T. C. T.; Hoeglund, A.; Baker, D. L. Virtual screening approaches for the identification of non-lipid autotaxin inhibitors. *Bioorg. Med. Chem.* **2008**, *16*, 1784–1795.
- (54) Fernandes, M. X.; Kairys, V.; Gilson, M. K. Comparing ligand interactions with multiple receptors via serial docking. *J. Chem. Inf. Comput. Sci.* **2004**, *44*, 1961–1970.
- (55) Kairys, V.; Fernandes, M. X.; Gilson, M. K. Screening drug-like compounds by docking to homology models: A systematic study. *J. Chem. Inf. Model.* **2006**, *46*, 365–379.
- (56) McGovern, S. L.; Shoichet, B. K. Information decay in molecular docking screens against holo, apo, and modeled conformations of enzymes. *J. Med. Chem.* **2003**, *46*, 2895–2907.
- (57) Huang, N.; Shoichet, B. K.; Irwin, J. J. Benchmarking sets for molecular docking. *J. Med. Chem.* **2006**, *49*, 6789–6801.
- (58) Ortiz, A. R.; Strauss, C. E. M.; Olmea, O. MAMMOTH (Matching molecular models obtained from theory): An automated method for model comparison. *Protein Sci.* **2002**, *11*, 2606–2621.
- (59) Marti-Renom, M. A.; Pieper, U.; Madhusudhan, M. S.; Rossi, A.; Eswar, N.; Davis, F. P.; Al-Shahrour, F.; Dopazo, J.; Sali, A. DBAli tools: mining the protein structure space. *Nucleic Acids Res.* **2007**, *35*, W393–W397.
- (60) Sali, A.; Blundell, T. L. Comparative protein modeling by satisfaction of spatial restraints. *J. Mol. Biol.* **1993**, *234*, 779–815.
- (61) Marti-Renom, M. A.; Madhusudhan, M. S.; Sali, A. Alignment of protein sequences by their profiles. *Protein Sci.* **2004**, *13*, 1071–1087.
- (62) Shen, M. Y.; Sali, A. Statistical potential for assessment and prediction of protein structures. *Protein Sci.* **2006**, *15*, 2507–2524.
- (63) Eramian, D.; Eswar, N.; Shen, M. Y.; Sali, A. How well can the accuracy of comparative protein structure models be predicted? *Protein Sci.* **2008**, *17*, 1881–1893.
- (64) Ferrin, T. E.; Huang, C. C.; Jarvis, L. E.; Langridge, R. The midas display system. *J. Mol. Graphics* **1988**, *6*, 13.
- (65) Kuntz, I. D.; Blaney, J. M.; Oatley, S. J.; Langridge, R.; Ferrin, T. E. A geometric approach to macromolecule–ligand interactions. *J. Mol. Biol.* **1982**, *161*, 269–288.
- (66) Lorber, D. M.; Shoichet, B. K. Hierarchical docking of databases of multiple ligand conformations. *Curr. Top. Med. Chem.* **2005**, *5*, 739–749.
- (67) Meng, E. C.; Shoichet, B. K.; Kuntz, I. D. Automated docking with grid-based energy evaluation. *J. Comput. Chem.* **1992**, *13*, 505–524.
- (68) Wei, B. Q. Q.; Baase, W. A.; Weaver, L. H.; Matthews, B. W.; Shoichet, B. K. A model binding site for testing scoring functions in molecular docking. *J. Mol. Biol.* **2002**, *322*, 339–355.
- (69) Jain, A. N.; Nicholls, A. Recommendations for evaluation of computational methods. *J. Comput.-Aided Mol. Des.* **2008**, *22*, 133–139.
- (70) Irwin, J. J.; Shoichet, B. K.; Mysinger, M. M.; Huang, N.; Colizzi, F.; Wassam, P.; Cao, Y. Automated docking screens: A feasibility study. *J. Med. Chem.* **2009**, *52*, 5712–5720.
- (71) Shapiro, S. S.; Wilk, M. B. An analysis of variance test for normality (complete samples). *Biometrika* **1965**, *52*, 591.
- (72) Marti-Renom, M. A.; Madhusudhan, M. S.; Fiser, A.; Rost, B.; Sali, A. Reliability of assessment of protein structure prediction methods. *Structure* **2002**, *10*, 435–440.
- (73) Wilcoxon, F. Individual comparisons by ranking methods. *Biometrics Bull.* **1945**, *1*, 80–83.
- (74) Ferrara, P.; Jacoby, E. Evaluation of the utility of homology models in high throughput docking. *J. Mol. Model.* **2007**, *13*, 897–905.
- (75) Laskowski, R. A. Surfnet - a Program for visualizing molecular surfaces, cavities, and intermolecular interactions. *J. Mol. Graphics* **1995**, *13*, 323–330.
- (76) Terasaka, T.; Nakanishi, I.; Nakamura, K.; Eikyu, Y.; Kinoshita, T.; Nishio, N.; Sato, A.; Kuno, M.; Seki, N.; Sakane, K. Structure-based de novo design of non-nucleoside adenosine deaminase inhibitors. *Bioorg. Med. Chem. Lett.* **2003**, *13*, 4147.
- (77) Terasaka, T.; Kinoshita, T.; Kuno, M.; Nakanishi, I. A highly potent non-nucleoside adenosine deaminase inhibitor: Efficient drug discovery by intentional lead hybridization. *J. Am. Chem. Soc.* **2004**, *126*, 34–35.
- (78) Prager, N. A.; Abendschein, D. R.; McKenzie, C. R.; Eisenberg, P. R. Role of thrombin compared with factor Xa in the procoagulant activity of whole-blood clots. *Circulation* **1995**, *92*, 962–967.
- (79) Brandstetter, H.; Kuhne, A.; Bode, W.; Huber, R.; vonderSaal, W.; Wirthensohn, K.; Engh, R. A. X-ray structure of active site-inhibited clotting factor Xa - Implications for drug design and substrate recognition. *J. Biol. Chem.* **1996**, *271*, 29988–29992.
- (80) Maignan, S.; Guilloteau, J. P.; Pouzieux, S.; Choi-Sledeski, Y. M.; Becker, M. R.; Klein, S. I.; Ewing, W. R.; Pauls, H. W.; Spada, A. P.; Mikol, V. Crystal structures of human factor Xa complexed with potent inhibitors. *J. Med. Chem.* **2000**, *43*, 3226–3232.
- (81) Brik, A.; Wong, C. H. HIV-1 protease: mechanism and drug discovery. *Org. Biomol. Chem.* **2003**, *1*, 5–14.
- (82) Baldwin, E. T.; Bhat, T. N.; Gulnik, S.; Liu, B. S.; Topol, I. A.; Kiso, Y.; Mimoto, T.; Mitsuya, H.; Erickson, J. W. Structure of Hiv-1 protease with Kni-272, a tight-binding transition-state analog containing allophenylboronate. *Structure* **1995**, *3*, 581–590.
- (83) Vonitzstein, M.; Wu, W. Y.; Kok, G. B.; Pegg, M. S.; Dyason, J. C.; Jin, B.; Phan, T. V.; Smythe, M. L.; White, H. F.; Oliver, S. W.; Colman, P. M.; Varghese, J. N.; Ryan, D. M.; Woods, J. M.; Bethell, R. C.; Hotham, V. J.; Cameron, J. M.; Penn, C. R. Rational design of potent sialidase-based inhibitors of influenza-virus replication. *Nature* **1993**, *363*, 418–423.
- (84) Abu Hammad, A. M.; Afifi, F. U.; Taha, M. O. Combining docking, scoring and molecular field analyses to probe influenza neuraminidase–ligand interactions. *J. Mol. Graphics Model.* **2007**, *26*, 443–456.
- (85) Bledsoe, R. K.; Madauss, K. P.; Holt, J. A.; Apolito, C. J.; Lambert, M. H.; Pearce, K. H.; Stanley, T. B.; Stewart, E. L.; Trump, R. P.; Willson, T. M.; Williams, S. P. A ligand-mediated hydrogen bond network required for the activation of the mineralocorticoid receptor. *J. Biol. Chem.* **2005**, *280*, 31283–31293.
- (86) Zhang, Z. M.; Olland, A. M.; Zhu, Y.; Cohen, J.; Berroddin, T.; Chippari, S.; Appavu, C.; Li, S.; Wilhelm, J.; Chopra, R.; Fensome, A.; Zhang, P. W.; Wrobel, J.; Unwalla, R. J.; Lyttle, R.; Winneker, R. C. Molecular and pharmacological properties of a potent and selective novel nonsteroidal progesterone receptor agonist tanaproget. *J. Biol. Chem.* **2005**, *280*, 28468–28475.
- (87) Egea, P. F.; Mitschler, A.; Moras, D. Molecular recognition of agonist ligands by RXRs. *Mol. Endocrinol.* **2002**, *16*, 987–997.
- (88) Teague, S. J. Implications of protein flexibility for drug discovery. *Nat. Rev. Drug Discovery* **2003**, *2*, 527–541.
- (89) Rester, U. Dock around the clock - Current status of small molecule docking and scoring. *QSAR Comb. Sci.* **2006**, *25*, 605–615.

- (90) Totrov, M.; Abagyan, R. Flexible ligand docking to multiple receptor conformations: a practical alternative. *Curr. Opin. Struct. Biol.* **2008**, *18*, 178–184.
- (91) Cozzini, P.; Kellogg, G. E.; Spyraakis, F.; Abraham, D. J.; Costantino, G.; Emerson, A.; Fanelli, F.; Gohlke, H.; Kuhn, L. A.; Morris, G. M.; Orozco, M.; Pertinhez, T. A.; Rizzi, M.; Sotriffer, C. A. Target flexibility: An emerging consideration in drug discovery and design. *J. Med. Chem.* **2008**, *51*, 6237–6255.
- (92) Teodoro, M. L.; Kavraki, L. E. Conformational flexibility models for the receptor in structure based drug design. *Curr. Pharm. Des.* **2003**, *9*, 1635–1648.
- (93) Jiang, F.; Kim, S. H. Soft docking - Matching of molecular-surface cubes. *J. Mol. Biol.* **1991**, *219*, 79–102.
- (94) Schnecke, V.; Swanson, C. A.; Getzoff, E. D.; Tainer, J. A.; Kuhn, L. A. Screening a peptidyl database for potential ligands to proteins with side-chain flexibility. *Proteins: Struct., Funct., Genet.* **1998**, *33*, 74–87.
- (95) Apostolakis, J.; Pluckthun, A.; Caffisch, A. Docking small ligands in flexible binding sites. *J. Comput. Chem.* **1998**, *19*, 21–37.
- (96) Leach, A. R. Ligand docking to proteins with discrete side-chain flexibility. *J. Mol. Biol.* **1994**, *235*, 345–356.
- (97) Jones, G.; Willett, P.; Glen, R. C.; Leach, A. R.; Taylor, R. Development and validation of a genetic algorithm for flexible docking. *J. Mol. Biol.* **1997**, *267*, 727–748.
- (98) Schaffer, L.; Verkhivker, G. M. Predicting structural effects in HIV-1 protease mutant complexes with flexible ligand docking and protein side-chain optimization. *Proteins: Struct., Funct., Genet.* **1998**, *33*, 295–310.
- (99) Anderson, A. C.; O'Neil, R. H.; Surti, T. S.; Stroud, R. M. Approaches to solving the rigid receptor problem by identifying a minimal set of flexible residues during ligand docking. *Chem. Biol.* **2001**, *8*, 445–457.
- (100) Althaus, E.; Kohlbacher, O.; Lenhof, H. P.; Muller, P. A combinatorial approach to protein docking with flexible side chains. *J. Comput. Biol.* **2002**, *9*, 597–612.
- (101) Kairys, V.; Gilson, M. K. Enhanced docking with the mining minima optimizer: Acceleration and side-chain flexibility. *J. Comput. Chem.* **2002**, *23*, 1656–1670.
- (102) Zavodszky, M. I.; Kuhn, L. A. Side-chain flexibility in protein-ligand binding: The minimal rotation hypothesis. *Protein Sci.* **2005**, *14*, 1104–1114.
- (103) Dinola, A.; Roccatano, D.; Berendsen, H. J. C. Molecular-dynamics simulation of the docking of substrates to proteins. *Proteins: Struct., Funct., Genet.* **1994**, *19*, 174–182.
- (104) Luty, B. A.; Wasserman, Z. R.; Stouten, P. F. W.; Hodge, C. N.; Zacharias, M.; Mccammon, J. A. A molecular mechanics grid method for evaluation of ligand–receptor interactions. *J. Comput. Chem.* **1995**, *16*, 454–464.
- (105) Wasserman, Z. R.; Hodge, C. N. Fitting an inhibitor into the active site of thermolysin: A molecular dynamics case study. *Proteins: Struct., Funct., Genet.* **1996**, *24*, 227–237.
- (106) Nakajima, N.; Higo, J.; Kidera, A.; Nakamura, H. Flexible docking of a ligand peptide to a receptor protein by multicanonical molecular dynamics simulation. *Chem. Phys. Lett.* **1997**, *278*, 297–301.
- (107) Pak, Y. S.; Wang, S. M. Application of a molecular dynamics simulation method with a generalized effective potential to the flexible molecular docking problems. *J. Phys. Chem. B* **2000**, *104*, 354–359.
- (108) Kua, J.; Zhang, Y. K.; Mccammon, J. A. Studying enzyme binding specificity in acetylcholinesterase using a combined molecular dynamics and multiple docking approach. *J. Am. Chem. Soc.* **2002**, *124*, 8260–8267.
- (109) Wu, G. S.; Robertson, D. H.; Brooks, C. L.; Vieth, M. Detailed analysis of grid-based molecular docking: A case study of CDOCKER - A CHARMM-based MD docking algorithm. *J. Comput. Chem.* **2003**, *24*, 1549–1562.
- (110) Camacho, C. J. Modeling side-chains using molecular dynamics improve recognition of binding region in CAPRI targets. *Proteins: Struct., Funct., Bioinform.* **2005**, *60*, 245–251.
- (111) Sivanesan, D.; Rajnarayanan, R. V.; Doherty, J.; Pattabiraman, N. In-silico screening using flexible ligand binding pockets: a molecular dynamics-based approach. *J. Comput.-Aided Mol. Des.* **2005**, *19*, 213–228.
- (112) Zhu, J.; Fan, H.; Liu, H. Y.; Shi, Y. Y. Structure-based ligand design for flexible proteins: Application of new F-DycoBlock. *J. Comput.-Aided Mol. Des.* **2001**, *15*, 979–996.
- (113) Krol, M.; Tournier, A. L.; Bates, P. A. Flexible relaxation of rigid-body docking solutions. *Proteins: Struct., Funct., Bioinform.* **2007**, *68*, 159–169.
- (114) Caffisch, A.; Fischer, S.; Karplus, M. Docking by Monte Carlo minimization with a solvation correction: Application to an FKBP-substrate complex. *J. Comput. Chem.* **1997**, *18*, 723–743.
- (115) Trosset, J. Y.; Scheraga, H. A. Flexible docking simulations: Scaled collective variable Monte Carlo minimization approach using Bezier splines, and comparison with a standard Monte Carlo algorithm. *J. Comput. Chem.* **1999**, *20*, 244–252.
- (116) Verkhivker, G. M.; Rejto, P. A.; Bouzida, D.; Arthurs, S.; Colson, A. B.; Freer, S. T.; Gehlhaar, D. K.; Larson, V.; Luty, B. A.; Marrone, T.; Rose, P. W. Parallel simulated tempering dynamics of ligand-protein binding with ensembles of protein conformations. *Chem. Phys. Lett.* **2001**, *337*, 181–189.
- (117) Claussen, H.; Buning, C.; Rarey, M.; Lengauer, T. FlexE: Efficient molecular docking considering protein structure variations. *J. Mol. Biol.* **2001**, *308*, 377–395.
- (118) Osterberg, F.; Morris, G. M.; Sanner, M. F.; Olson, A. J.; Goodsell, D. S. Automated docking to multiple target structures: Incorporation of protein mobility and structural water heterogeneity in AutoDock. *Proteins: Struct., Funct., Bioinform.* **2002**, *46*, 34–40.
- (119) Ferrari, A. M.; Wei, B. Q.; Costantino, L.; Shoichet, B. K. Soft docking and multiple receptor conformations in virtual screening. *J. Med. Chem.* **2004**, *47*, 5076–5084.
- (120) Wei, B. Q.; Weaver, L. H.; Ferrari, A. M.; Matthews, B. W.; Shoichet, B. K. Testing a flexible-receptor docking algorithm in a model binding site. *J. Mol. Biol.* **2004**, *337*, 1161–1182.
- (121) Cavasotto, C. N.; Abagyan, R. A. Protein flexibility in ligand docking and virtual screening to protein kinases. *J. Mol. Biol.* **2004**, *337*, 209–225.
- (122) Knegtel, R. M. A.; Kuntz, I. D.; Oshiro, C. M. Molecular docking to ensembles of protein structures. *J. Mol. Biol.* **1997**, *266*, 424–440.
- (123) Damm, K. L.; Carlson, H. A. Exploring experimental sources of multiple protein conformations in structure-based drug design. *J. Am. Chem. Soc.* **2007**, *129*, 8225–8235.
- (124) Lin, J. H.; Perryman, A. L.; Schames, J. R.; Mccammon, J. A. Computational drug design accommodating receptor flexibility: The relaxed complex scheme. *J. Am. Chem. Soc.* **2002**, *124*, 5632–5633.
- (125) Lin, J. H.; Perryman, A. L.; Schames, J. R.; Mccammon, J. A. The relaxed complex method: Accommodating receptor flexibility for drug design with an improved scoring scheme. *Biopolymers* **2003**, *68*, 47–62.
- (126) Mccammon, J. A. Target flexibility in molecular recognition. *Biochim. Biophys. Acta: Proteins Proteomics* **2005**, *1754*, 221–224.
- (127) Wong, C. F.; Kua, J.; Zhang, Y. K.; Straatsma, T. P.; Mccammon, J. A. Molecular docking of balanol to dynamics snapshots of protein kinase A. *Proteins: Struct., Funct., Bioinform.* **2005**, *61*, 850–858.
- (128) Pang, Y. P.; Kozikowski, A. P. Prediction of the binding sites of huperzine-a in acetylcholinesterase by docking studies. *J. Comput.-Aided Mol. Des.* **1994**, *8*, 669–681.
- (129) Gorfe, A. A.; Caffisch, A. Functional plasticity in the substrate binding site of beta-secretase. *Structure* **2005**, *13*, 1487–1498.
- (130) Broughton, H. B. A method for including protein flexibility in protein-ligand docking: Improving tools for database mining and virtual screening. *J. Mol. Graphics Model.* **2000**, *18*, 247.
- (131) Cavasotto, C. N.; Kovacs, J. A.; Abagyan, R. A. Representing receptor flexibility in ligand docking through relevant normal modes. *J. Am. Chem. Soc.* **2005**, *127*, 9632–9640.
- (132) Meiler, J.; Baker, D. ROSETTALIGAND: Protein-small molecule docking with full side-chain flexibility. *Proteins: Struct., Funct., Bioinform.* **2006**, *65*, 538–548.
- (133) Sherman, W.; Day, T.; Jacobson, M. P.; Friesner, R. A.; Farid, R. Novel procedure for modeling ligand/receptor induced fit effects. *J. Med. Chem.* **2006**, *49*, 534–553.
- (134) Feher, M. Consensus scoring for protein-ligand interactions. *Drug Discovery Today* **2006**, *11*, 421–428.

CI9003706